RSC Medicinal Chemistry

ROYAL SOCIETY OF CHEMISTRY

RESEARCH ARTICLE

Cite this: *RSC Med. Chem.*, 2023, **14**, 2625

A silicon-containing aryl/penta-1,4-dien-3-one/amine hybrid exhibits antiproliferative effects on breast cancer cells by targeting the HSP90 C-terminus without inducing heat-shock response†

Yu-Ting Liao,‡[a] Xin-Ye Du,‡[ab] Mei Wang,‡[a] Chun-Xia Zheng,[a] Dashan Li,[a] Chuan-Huizi Chen,[a] Rong-Tao Li*[b] and Li-Dong Shao *[a]

A pharmacophore-hybridized strategy based on previously reported HSP90 C-terminal inhibitors was utilized to prepare 32 aryl/penta-1,4-dien-3-one/amine hybrids. Among them, a silicon-containing compound **1z** exhibited remarkable broad-spectrum antiproliferative effects on various human breast cancer cell lines. Through fluorescence polarization and AlphaScreen-based assays, we demonstrated that **1z** specifically inhibited the HSP90 C-terminus without affecting HSP90 N-terminus. Furthermore, **1z** effectively inhibited the HSP90 C-terminus without inducing heat-shock response (HSR), leading to the degradation of its client proteins HER2, pAKT, AKT, and CDK4, causing G_1 arrest of MCF-7 and SKBr3 cells, and ultimately contributing to apoptosis of these cells through caspase-3, caspase-8, and caspase-9 activation. Additionally, the penta-1,4-dien-3-one linker in the hybrid, a large bulky lipophilic substitution in the aryl fragment at the 3′-site, and the presence of *N*-methylpiperazine as the amine fragment were identified as crucial factors that significantly contributed to the observed antiproliferative activity through structure–activity relationship (SAR) analysis. Lastly, we found that **1z** exhibited superior thermostability compared to vibsanin B derivatives and good *in vitro* metabolic stability in simulated intestinal fluid, representing one of the few reported silicon-containing HSP90 C-terminal inhibitors.

Received 23rd August 2023,
Accepted 11th October 2023

DOI: 10.1039/d3md00431g

rsc.li/medchem

Introduction

Cancer is one of the most fatal diseases that endanger human life. There were about 19.3 million new cases of cancer worldwide in 2020, of which 10 million deaths were mostly found in developing countries, and unfortunately the number is increasing quickly.[1] Breast cancer is currently the leading cause of cancer-related deaths in women.[2–4] Although there are targeted therapeutic agents available for different subtypes of breast cancer, such as trastuzumab and pertuzumab for HER2-positive subtypes, olaparib for PARP inhibition, alpelisib for PI3K inhibition, and AKT inhibitors, these treatments may not fully meet the needs of all patients.[5,6] Heat shock protein 90 (HSP90), an ATP-dependent molecular chaperone, is responsible for the conformational maturation, activation, and stability of more than 200 client proteins involved in signal transduction which is essential for hallmarks of cancer and drug resistance development. In eukaryotic cells, HSP90 is upregulated from its native content of 1% to 5% only under cellular stress and is continuously overexpressed in cancerous cells but not in normal cells. Thus, HSP90 inhibitors offer a promising approach to treating breast cancer by targeting the HSP90 protein and degrading its client proteins (including HER2, PI3K, and AKT, *etc.*), resulting in a multi-faceted attack on cancer cells.[7] Geldanamycin-, radicicol-, and novobiocin-based derivatives are representative examples of HSP90 inhibitors that have shown high potential in treating various subtypes of breast cancer, and some are already undergoing clinical studies.[8–13]

A range of structurally designed HSP90 inhibitors with remarkable properties have been reported during the past two decades. Notably, HSP90 C-terminal and HSP90 isoform-selective inhibitors have emerged as current hotspots for HSP90 inhibitors due to their outstanding functions in molecular biology.[10,11,14] These inhibitors have exhibited potent antiproliferative activity against various breast cancer cell lines. Blagg *et al.* carried out a landmark medicinal chemistry on the

[a] *Yunnan Key Laboratory of Southern Medicinal Resources, School of Chinese Materia Medica, Yunnan University of Chinese Medicine, Kunming, 650500, China. E-mail: shaolidong@ynutcm.edu.cn*
[b] *Faculty of Life Science and Technology, Kunming University of Science and Technology, Kunming, 650500, China. E-mail: rongtaolikm@163.com*
† Electronic supplementary information (ESI) available. See DOI: https://doi.org/10.1039/d3md00431g
‡ These authors contributed equally.

natural product novobiocin and systematically developed various novobiocin-based HSP90 C-terminal inhibitors that exhibited a great potency towards HER2-positive breast cancer.[8,15–29] Lee and coworkers successfully designed and synthesized a series of deguelin-based HSP90 C-terminal inhibitors, which demonstrated excellent antiproliferative activity against different subtypes of breast cancer cell lines, especially the trastuzumab-resistant HER2-positive breast cancer.[5,6,30–35] McAlpine and coworkers uncovered the effects of San A-amide-based derivatives on HSP90 C-terminal interactions with its clients IP6K2, FKBP38, FKBP52, and HOP through the binding to the HSP90 N/M-terminus, which represented novel HSP90 C-terminal allosteric modulators.[36–40] Very recently, a covalent inhibitor binding to Cys598 on the Hsp90 C-terminus and exhibiting antiproliferative activities against a lot of cancer cells without inhibiting ATPase activity was reported by Xu and co-workers, which gave new insights into the exploration of HSP90 C-terminal inhibition and HSP90 functions.[41] Nevertheless, the limited scaffolds for HSP90 C-terminal inhibitors remain to be investigated. In a previous study, we demonstrated that the natural product vibsanin B and its analogue VB4157 showed impressive HSP90 C-terminal inhibitory activity and antiproliferative activities against various breast cancer cell lines.[42] However, besides the induction of heat-shock response (HSR), the thermostability of these derivatives remains a concern; the time for 50% decomposition in boiling toluene (120 °C) of these derivatives was estimated to be shorter than 5 min due to the oxy-Cope rearrangement.[42,43] To address this issue, we aimed to create a structurally simplified and thermostable scaffold inspired by vibsanin B and other well-established HSP90 C-terminal inhibitors[44,45] (Fig. 1) by retaining the α,β-unsaturated ketone fragment as a linker and connecting its two ends to the frequently occurring pharmacophores of HSP90 C-terminal inhibitors to form an aryl/penta-1,4-dien-3-one/amine chimera. Thus, this article focuses on the design and synthesis of a series of aryl/penta-1,4-dien-3-one/amine hybrids as a novel generation of thermostable HSP90 C-terminal inhibitors without HSR induction.

Results and discussion

Design and synthesis of aryl/penta-1,4-dien-3-one/amine hybrids 1

Inspired by previously published HSP90 C-terminal inhibitors (Fig. 1), the aryl groups (like the green parts in curcumin,[44] SH-1242, carboxamide, EGCG, and others[10]), the α,β-unsaturated ketone fragments (like the red parts in curcumin, vibsanin B, VB4157, and others[10]), and the tertiary amines (like the blue parts in VB4157, carboxamide, and others[10]) are key pharmacophores and frequently presented. We envisioned that a new scaffold for HSP90 C-terminal inhibitors might be readily obtained through the combination of these key fragments. Therefore, we used the α,β-unsaturated ketone fragment as a linker and connected its two ends to the aryl part and amine part to form an aryl/penta-1,4-dien-3-one/amine chimera. The synthetic route to aryl/penta-1,4-dien-3-one/amine hybrids **1** features a two-step facile transformation including Michael addition and aldol reaction of enone **2** with amines **3** and aryl aldehydes **4** (Scheme 1). Namely, enamines **5** were readily prepared through the Michael addition of amines **3** to enone **2** in the presence of 6 N NaOH (Scheme 1, path a). Subsequently, aldol reaction of enamines **5a–5f** with a series of aryl aldehydes **4** were realized by a strong base lithium hexamethyldisilazide (LiHMDS) (Scheme 1, path b). As a result, 32 hybrids (**1a–1af**) bearing various aryls and amines were successfully prepared in 20–78% yields by this strategy (Scheme 2).

Biological evaluation of aryl/penta-1,4-dien-3-one/amine hybrids

After obtaining the hybrids **1**, the inhibitory ratio of hybrids **1a–1af** against the proliferation of MCF-7 human breast cancer cell lines was then tested at a dose of 20 μM. The

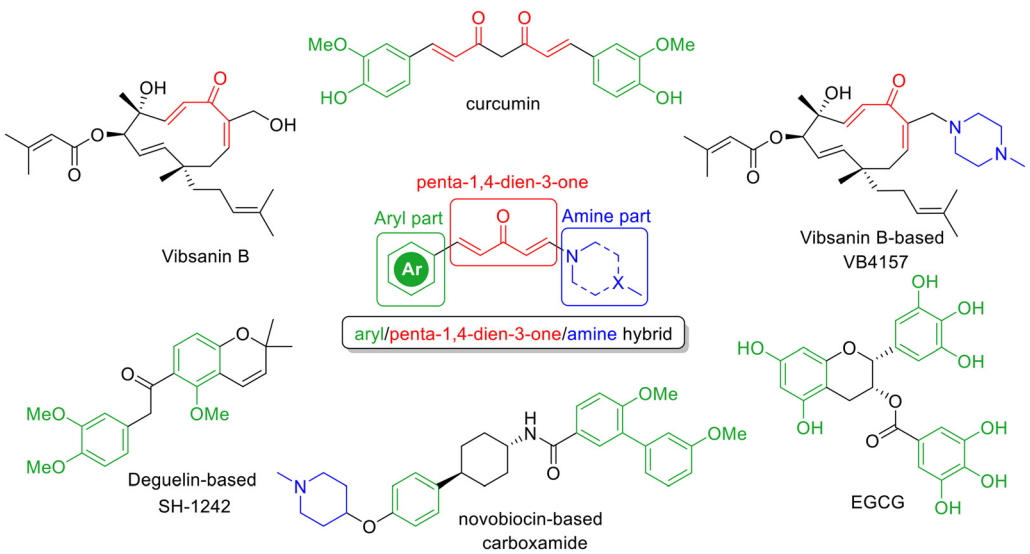

Fig. 1 Selected HSP90 C-terminal inhibitors and the proposed hybrid.

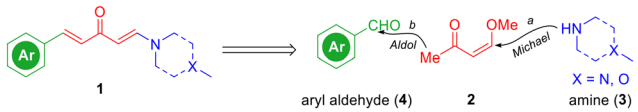

Scheme 1 Retrosynthetic analysis of aryl/penta-1,4-dien-3-one/amine hybrids **1**.

results demonstrated that hybrids **1o**, **1p**, **1z**, and **1ac** exhibited significant inhibitory effects on the growth of MCF cell lines at a concentration of 20 μM, with all inhibitory rates above 50% (***$p < 0.001$, Fig. 2). Further determination of their half-inhibitory concentrations (IC_{50}) against the growth of MCF cell lines revealed that compound **1z** (IC_{50} = 7.85 μM) exhibited greater potency than the other three compounds (IC_{50} values ranging from 12.86 to 16.71 μM) and was more potent than the positive control cisplatin (DDP) and novobiocin (NB, IC_{50} = 205 μM, Fig. S1†) but less potent than geldanamycin (GA) (Table 1). Subsequently, we assessed the inhibitory effects of **1z** on the growth of five distinct breast cancer cell lines (HCC1806, MDA-MB-231, MDA-MB-

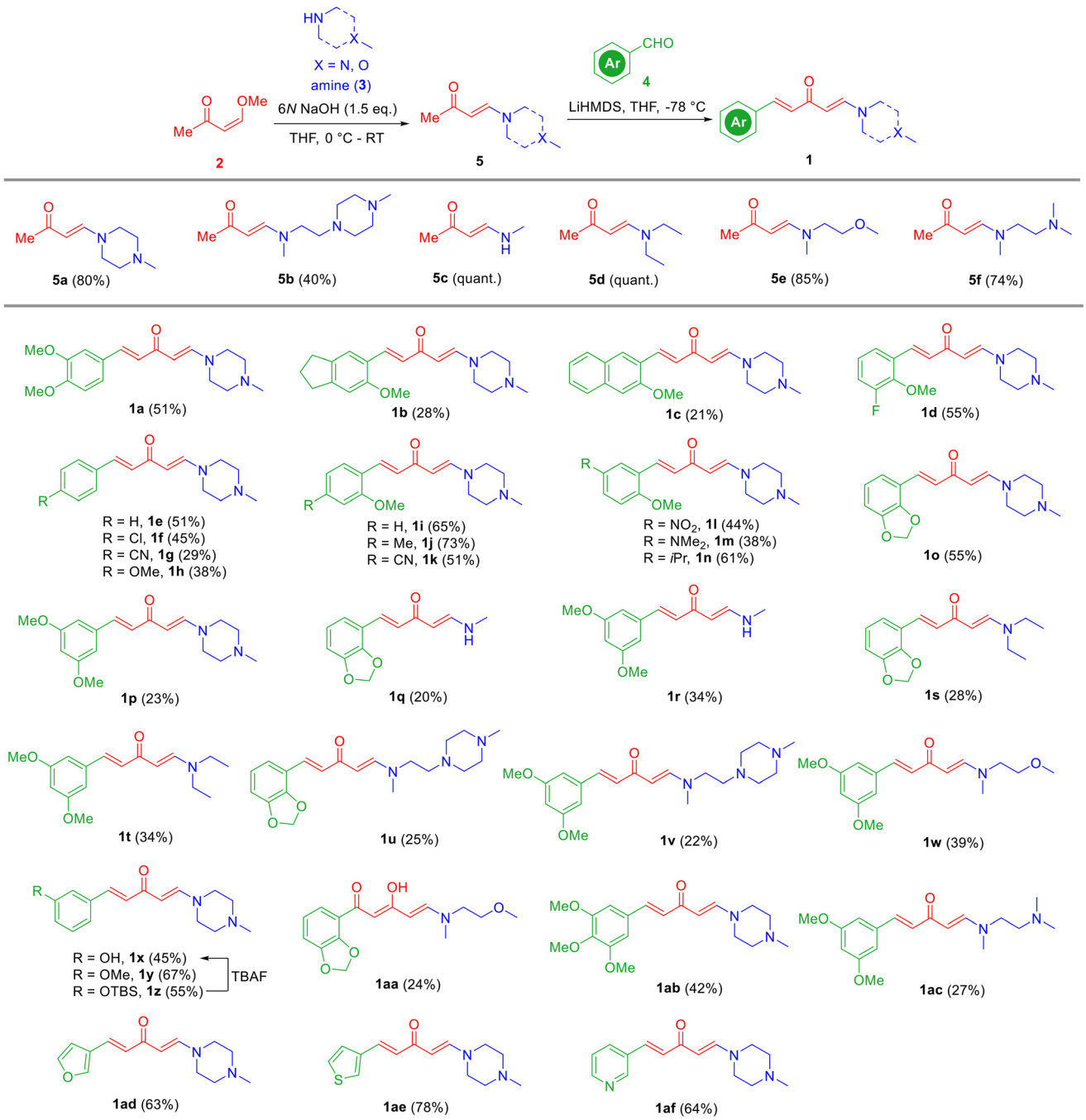

Scheme 2 Synthesis of aryl/penta-1,4-dien-3-one/amine hybrids **1**.

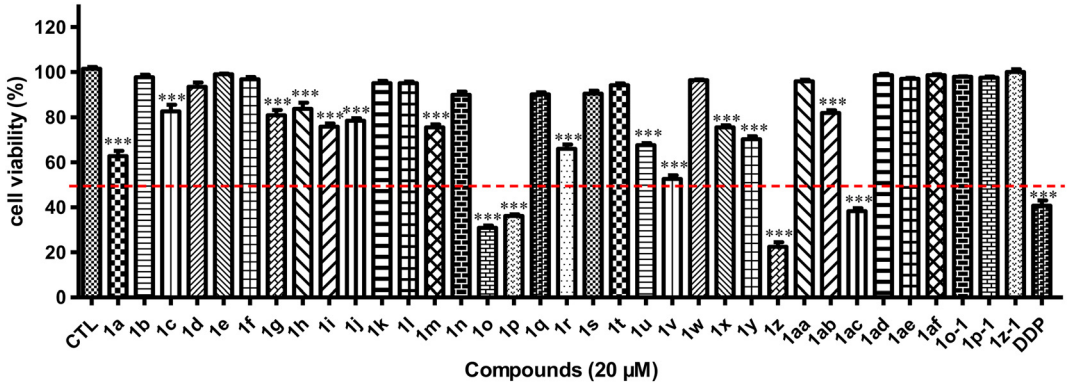

Fig. 2 Cell viability of MCF-7 cells after treating with hybrids **1** (20 μM), DMSO (CTL), and DDP (20 μM) [***$p < 0.001$ *vs.* CTL, $n = 3$].

468, SKBr3, and BT474) and observed its wide range of antiproliferative activities against these breast cancer cell lines (IC_{50} values ranging from 8.16 to 12.14 μM).

Molecular modelling

To gain more insights into the correlation of **1z** with the HSP90 C-terminus, we conducted molecular simulation experiments (Fig. 3). The blind docking results demonstrated that **1z** can access the HSP90 C-terminal dimerization region comprising the pocket formed by the H4, H5, H4′, and H5′ helices[46,47] with an unfolded *E*,*E*-conformation. In detail, the N atom of *N*-methylpiperazine in the amine fragment of **1z** forms a robust salt bridge with the amino acid residue ASP656, while the aryl fragment of **1z** establishes significant lipophilic interactions with amino acid residues in H4′, H5′, and H5. Specifically, there is a π–δ interaction between ARG690 and the aromatic ring of **1z**, alkyl–alkyl interactions involving LEU662, MET691, LEU694, and GLY695 from H4′/H5′ as well as LEU695 and LEU696 from H5 with the *tert*-butyldimethyl silyl (TBS) fragment in **1z**, which contributed to the lipophilic interactions.[48] These interactions provide a valuable support for the superior performance of **1z** compared to other derivatives.

Structure–activity relationships

Based on the aforementioned information, the SARs for the antiproliferative activities of aryl/penta-1,4-dien-3-one/amine hybrids **1** against breast cancer cells could be summarized as follows (Fig. 4): (i) the presence of a penta-1,4-dien-3-one linker which most likely maintained the *E*,*E*-conformation of the hybrids is necessary for activity, as observed in **1o** *vs.* **1o-1**, **1p** *vs.* **1p-1**, and **1z** *vs.* **1z-1** (Fig. 2 and Scheme S1†); (ii) substituting the 3′-site of the aryl fragment with a bulky lipophilic group like the TBS group (**1z**) is highly favorable for antiproliferative activity. Additionally, combining substitution at the 3′-site with that in other sites, such as 2′,3′-dioxymethylene (**1o**) and 3′,5′-dimethoxy (**1p**), also enhances antiproliferative activity; (iii) the amine fragment, particularly that with a less flexible N–CH_2–CH_2–N moiety like *N*-methylpiperazine, exhibits the highest activity.

Biological evaluation of 1z

To ascertain whether the designed synthetic derivatives function as HSP90 inhibitors, the most potent compound **1z** was chosen among them and its impact on HSP90, HSP70, and several crucial HSP90 client proteins in MCF-7 and SKBr3 cells was assessed. The results demonstrated that **1z** downregulated HSP90 client proteins HER2, pAKT, and CDK4, but did not affect the expression level of AKT in MCF-7 cells (Fig. 5A), while these biomarkers could be significantly downregulated by **1z** in SKBr3 cells (Fig. 5A). The expression of HSP90 and HSP70 was less impacted by **1z** compared to GA, which exhibited similarities to NB in both cells. Subsequent enzyme-based experiments revealed that **1z** lacked binding capacity to the HSP90 N-terminus (Fig. 5B), whereas it could disturb the binding of Cyp40 with the recombined HSP90 C-terminus with an IC_{50} value of 53.94 μM (Fig. 5C), surpassing NB in terms of inhibitory potency

Table 1 Antiproliferative activities of hybrids against breast cancer cell lines (IC_{50}, μM)[a]

Compd	MCF-7	HCC1806	MDA-MB-231	MDA-MB-468	SKBr3	BT474
1o	12.86 ± 1.05	13.20 ± 0.74	8.14 ± 0.66	>20	ND	ND
1p	14.20 ± 1.04	14.80 ± 0.70	9.13 ± 0.68	>20	ND	ND
1z	7.85 ± 0.09	10.10 ± 1.21	11.70 ± 1.60	8.16 ± 0.07	12.14 ± 1.05	9.06 ± 0.07
1ac	16.71 ± 1.03	14.70 ± 1.90	12.90 ± 2.21	>20	ND	ND
GA[b]	0.13 ± 0.01	0.12 ± 0.01	0.15 ± 0.02	0.033	0.033	0.027
DDP[b]	15.66 ± 1.03	2.14 ± 0.02	32.57 ± 1.72	2.31 ± 0.05	4.34 ± 0.27	11.03 ± 0.78

[a] Data were determined as mean ± SD from three independent experiments. [b] Positive control.

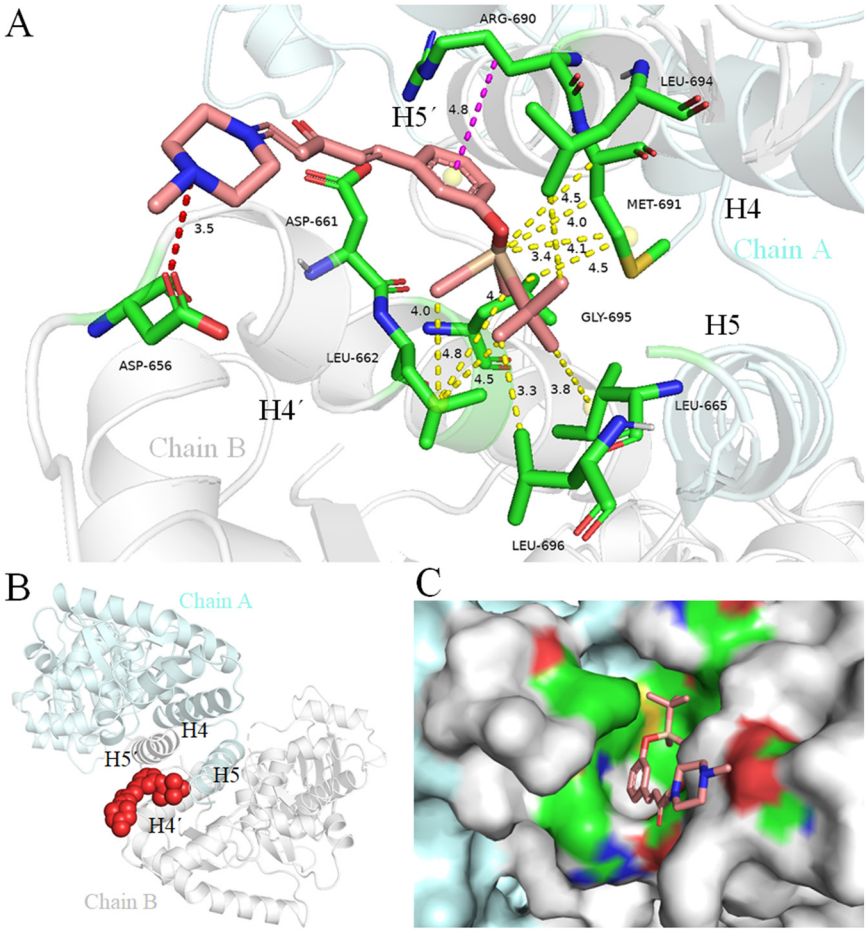

Fig. 3 Predicted binding mode of **1z** in the HSP90 C-terminus. (A) Interactions between **1z** (pink) with the amino acids (green) of H4′, H5′, and H5 in the HSP90 C-terminus (PDB 3Q6M), chain A (cyan), chain B (gray), salt bridge: red-dotted line; π–δ interaction: purple-dotted line; alkyl–alkyl interactions: yellow-dotted line. (B) A global view of binding mode; **1z** is depicted in a red space filling model. (C) Solid surface map of the interaction pocket with compound **1z**; red, blue, and green colored regions correspond to negatively charged, positively charged, and neural areas, respectively.

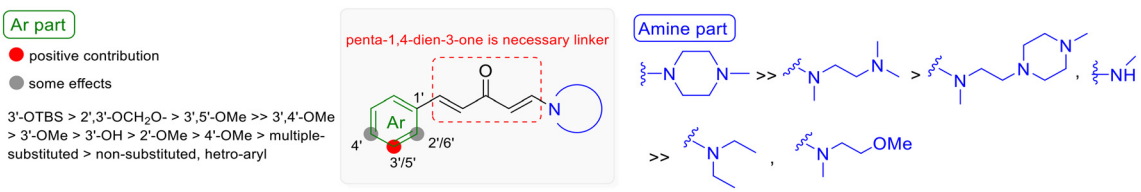

Fig. 4 The structure–activity relationships of hybrids **1**.

(IC_{50} = 82.43 μM), further corroborating our docking results of **1z** interacting with the HSP90 C-terminus (Fig. 3). Furthermore, considering that the majority of HSP90 C-terminal inhibitors are not associated with heat shock response (HSR) due to their incapacity to promote the prosurvival factor HSP70,[49,50] our investigation revealed that **1z** does not elevate the expression levels of HSP70 in both MCF-7 and SKBr3 cells (Fig. 5A), thus suggesting its unlikelihood to induce HSR effects. Consequently, a cellular immunofluorescence experiment was performed and confirmed that **1z** almost did not induce the alterations in HSP70 levels in MCF-7 and SKBr3 cells compared to GA (Fig. 6). To further address whether the unchanged HSP70 levels resulted from the inactivated upstream HSF-1/HSP90 axis, cellular immunofluorescence of HSF-1 in MCF-7 and SKBR3 cells was also performed. We found that **1z** apparently precluded the nuclear accumulation of HSF-1 in both MCF-7 and SKBR3 cells (Fig. 6). Taken together, it can be inferred that **1z** functions as a prototypical HSP90 C-terminal inhibitor without HSR induction.

Subsequently, we investigated the distribution of the cell population in different stages of the cell cycle. Flow cytometric analyses were performed with MCF-7 and SKBr3 cells. As a result, **1z** elevated the population of MCF-7 and

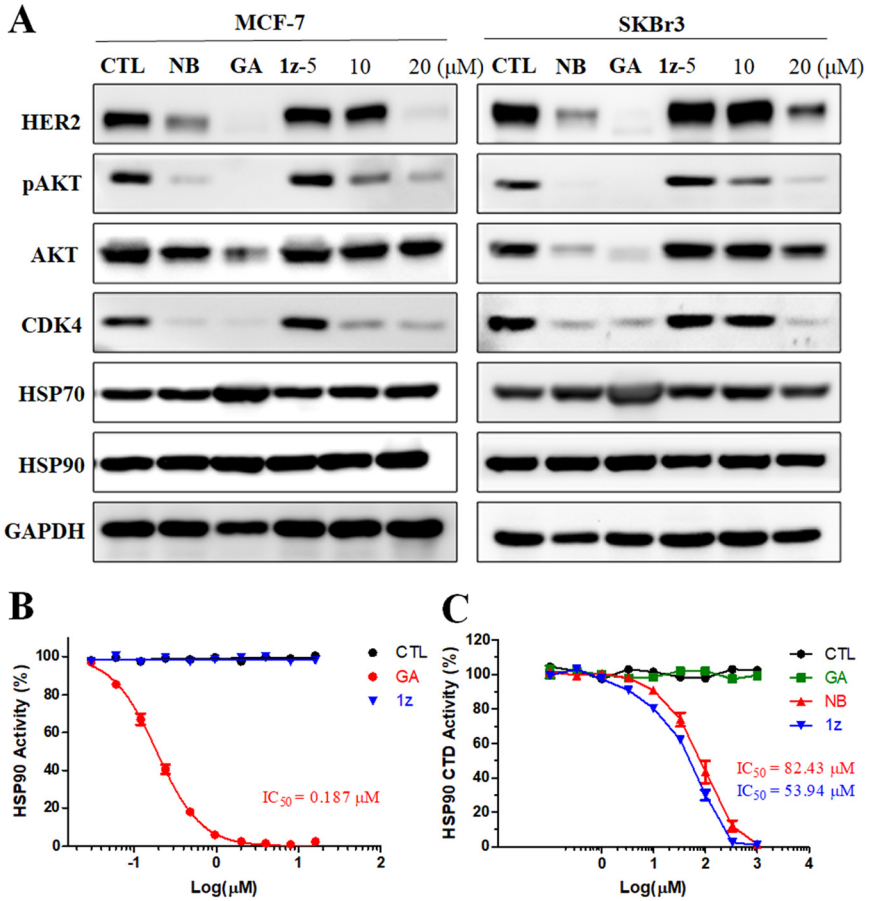

Fig. 5 Effects of **1z** on HSP90 and its client proteins in MCF-7 and SKBr3 cells. (A) Western blotting analysis of HER2, pAKT, AKT, CDK4, HSP70, and HSP90 protein expression in MCF-7 and SKBr3 cells after treatments with CTL (DMSO), GA (1.25 μM), NB (700 μM), and compound **1z** (5, 10, and 20 μM) for 48 h. GAPDH was used as a loading control. (B) Unlike GA, **1z** cannot compete the binding of FITC-GA (5 nM) with HSP90 in fluorescence polarization. (C) AlphaScreen-based HSP90 C-terminal inhibitory activities of **1z**, GA, and NB (the results were determined by two dependent experiments).

SKBr3 cells in the G_1 phase (***$p < 0.001$, Fig. 7A and B). Interestingly, **1z** could induce obvious apoptosis of both cancer cells but in different manners, of which a late-stage apoptosis of MCF-7 cells and an early-stage apoptosis of SKBr3 cells were observed after treatments with **1z** (0–20 μM) for 36 h (Fig. 7A and B). Furthermore, proteolytic activation of caspase-3, -8, and -9 was detected in **1z**-teated MCF-7 and SKBr3 cells, respectively (Fig. 7C and D). The cleavage of pro-caspase-8 in MCF-7 cells and pro-caspase-3, -8, and -9 in SKBr3 cells as well as the cleavage of PARP in both cells was increased after **1z** treatment. These observations suggested that **1z** could induce cell cycle arrest and apoptosis, thereby resulting in its antiproliferative effects.

Thermostability, *in vitro* metabolic stability, and preliminary toxicity study

Previous work has indicated the thermal instability of vibsanin B derivatives. Despite some improvement in the thermal stability of VB4157 compared to vibsanin B,[42] it fails to meet the prerequisites for comprehensive development. In this study, we eliminated the oxy-Cope rearrangement system in vibsanin B,[43] which is responsible for its thermo-instability. Consequently, we developed and synthesized aryl/penta-1,4-dien-3-one/amine hybrids **1**, aiming to fundamentally address the issue of thermo-instability. Subsequently, we examined the thermal stability of **1z** in boiling toluene and found it was stable for approximately 12 hours at 120 °C. After 12 hours, the TBS moiety began to be removed, resulting in the formation of **1x** (Fig. 8A). Nonetheless, the thermal stability of **1z** (time for 50% decomposition > 12 hours) has shown a qualitative improvement compared to VB4157 (time for 50% decomposition <5 min). Moreover, the *in vitro* metabolic stability of **1z** in simulated intestinal fluid was also tested (Fig. 8B). It was shown that **1z** was stable at least for 1 hour in simulated intestinal fluid but unstable in simulated gastric fluid (data not shown). In addition, the preliminary toxicity of **1z** was also tested using human embryonic kidney cells (293T).[51] As a result, **1z** [IC_{50} = 32.65 μM, selectivity index (SI) towards MCF-7: ~4.2] was less toxic than both DDP (IC_{50} = 10.81 μM) and GA (IC_{50} = 0.53 μM), but more toxic than NB

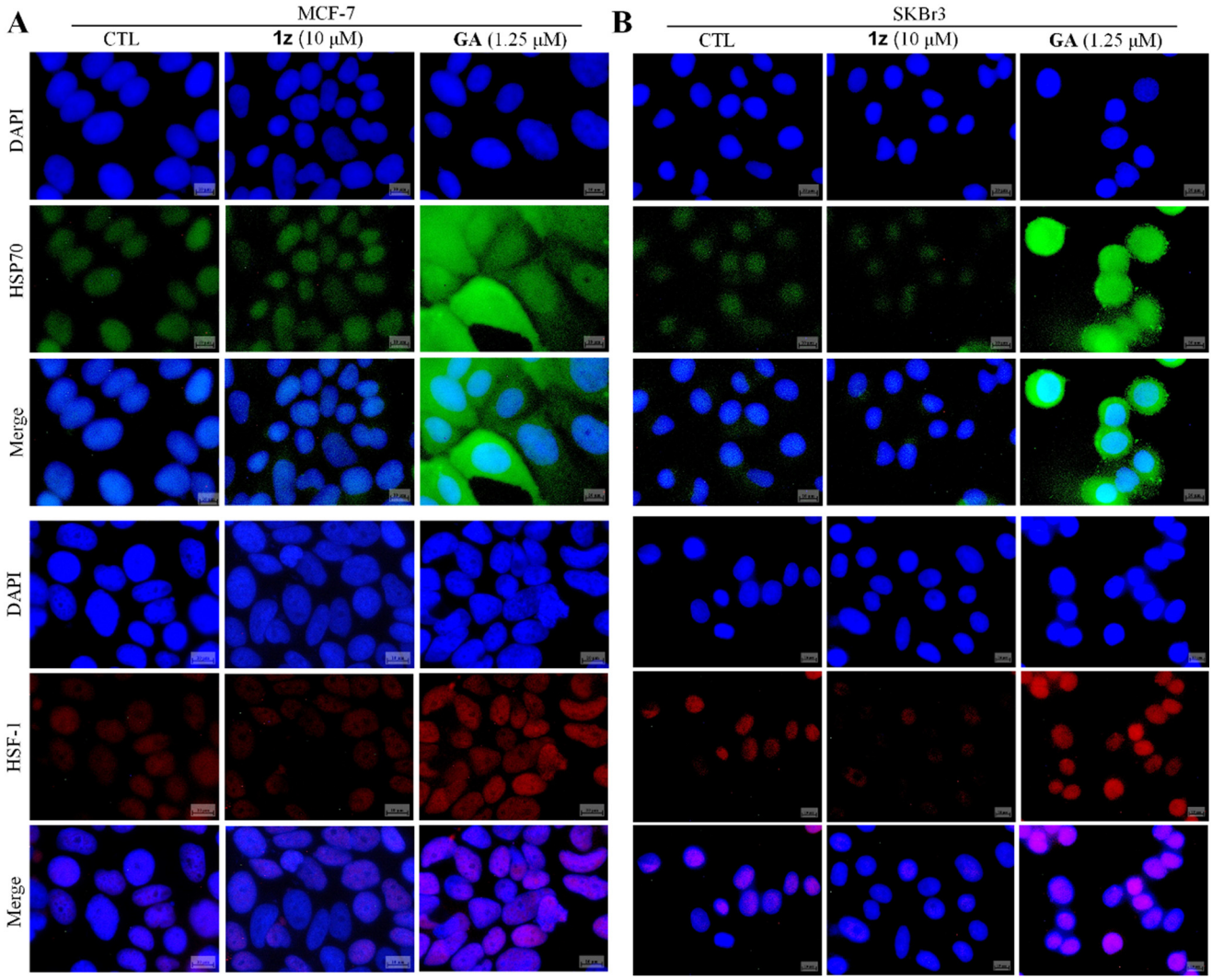

Fig. 6 Hybrid **1z** does not induce HSR. (A) MCF-7 and (B) SKBr3 cells were treated with CTL (DMSO), **1z** (10 μM), and GA (1.25 μM) for 36 h and then immunostained with HSP70 (green), HSF-1 (red), and DAPI (blue). Scale bar: 10 μm.

(IC_{50} > 100 μM, data not shown) (Fig. S1†), thereby establishing a foundation for subsequent optimization of this category of HSP90 inhibitors.

Conclusions

In conclusion, we have successfully designed and synthesized a novel class of aryl/penta-1,4-dien-3-one/amine hybrids as inhibitors targeting the HSP90 C-terminus. Among these hybrids, compound **1z** showed significant antiproliferative effects on various human breast cancer cell lines, including MCF-7, HCC1806, MDA-MB-231, MDA-MB-468, SKBr3, and BT474. Furthermore, our findings revealed that **1z** effectively suppressed the C-terminal activity of HSP90, resulting in the degradation of HSP90 client proteins HER2, pAKT, AKT, and CDK4, without inducing HSR. Consequently, by HSP90 inhibition, **1z** induced cell cycle arrest and ultimately led to cell apoptosis through the activation of caspase-3, caspase-8, and caspase-9. Subsequent SARs analysis, complemented by molecular simulation, and cellular and enzyme-based experiments, highlighted the critical contributions of the penta-1,4-dien-3-one linker in the hybrid, the presence of a large bulky lipophilic silyl substitution at the 3′-site of the aryl fragment, and the inclusion of *N*-methylpiperazine in the amine fragment. These factors significantly influenced the observed antiproliferative activity. Additionally, **1z** exhibited enhanced thermostability compared to vibsanin B derivatives and good *in vitro* metabolic stability in simulated intestinal fluid, representing one of the few silicon-containing HSP90 C-terminal inhibitors reported to date. These comprehensive findings provide a scientific foundation for the future development of HSP90C-terminal inhibitors.

Experimental section

Chemistry

General. All reactions were carried out under an atmosphere of argon in an oven-dried flask, and were

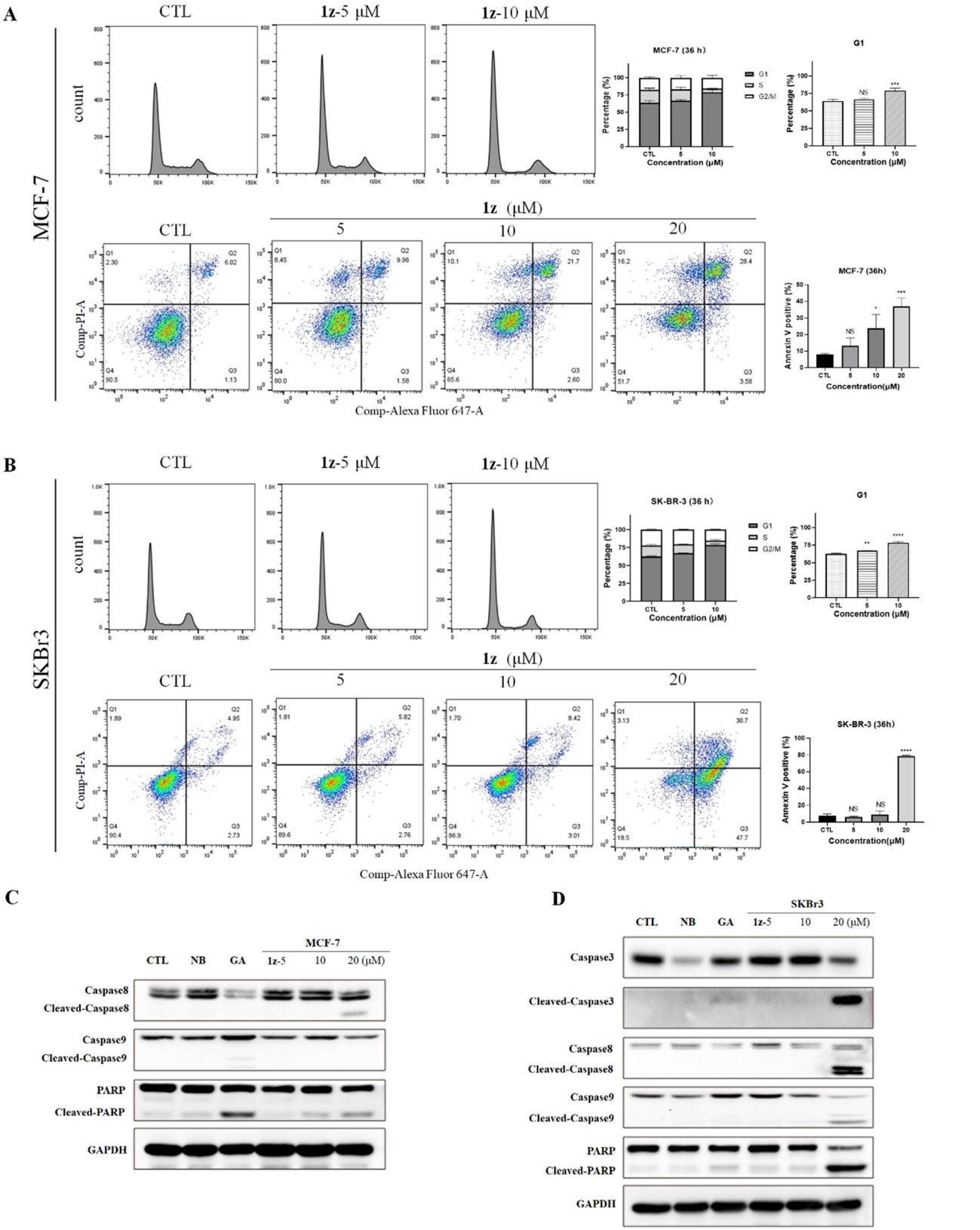

Fig. 7 Hybrid **1z** induced cell cycle arrest and apoptosis of MCF-7 and SKBr3 cells. (A) MCF-7 and (B) SKBr3 cells were treated with **1z** (0, 5, and 10 μM) for 36 h and stained with PI; cell cycle distribution was tested by flow cytometry. G_1 population changes in cell cycle distribution (**$p < 0.01$, ***$p < 0.001$ *vs.* CTL, $n = 3$). Annexin V/PI staining was used to determine the early and late apoptotic cells after treating with **1z** (0, 5, 10, and 20 μM) for 36 h (*$p < 0.05$, ***$p < 0.001$ *vs.* CTL, $n = 3$). (C) Effects of CTL (DMSO), NB (700 μM), GA (1.25 μM), and **1z** (5–20 μM, 48 h) on expression of caspase-8, caspase-9, cleaved-caspase-8, cleaved-caspase-9, PARP, and cleaved-PARP in MCF-7 cells, and on expression of caspase-3, cleaved-caspase-3, caspase-8, caspase-9, cleaved-caspase-8, cleaved-caspase-9, PARP, and cleaved-PARP in SKBr3 cells (D).

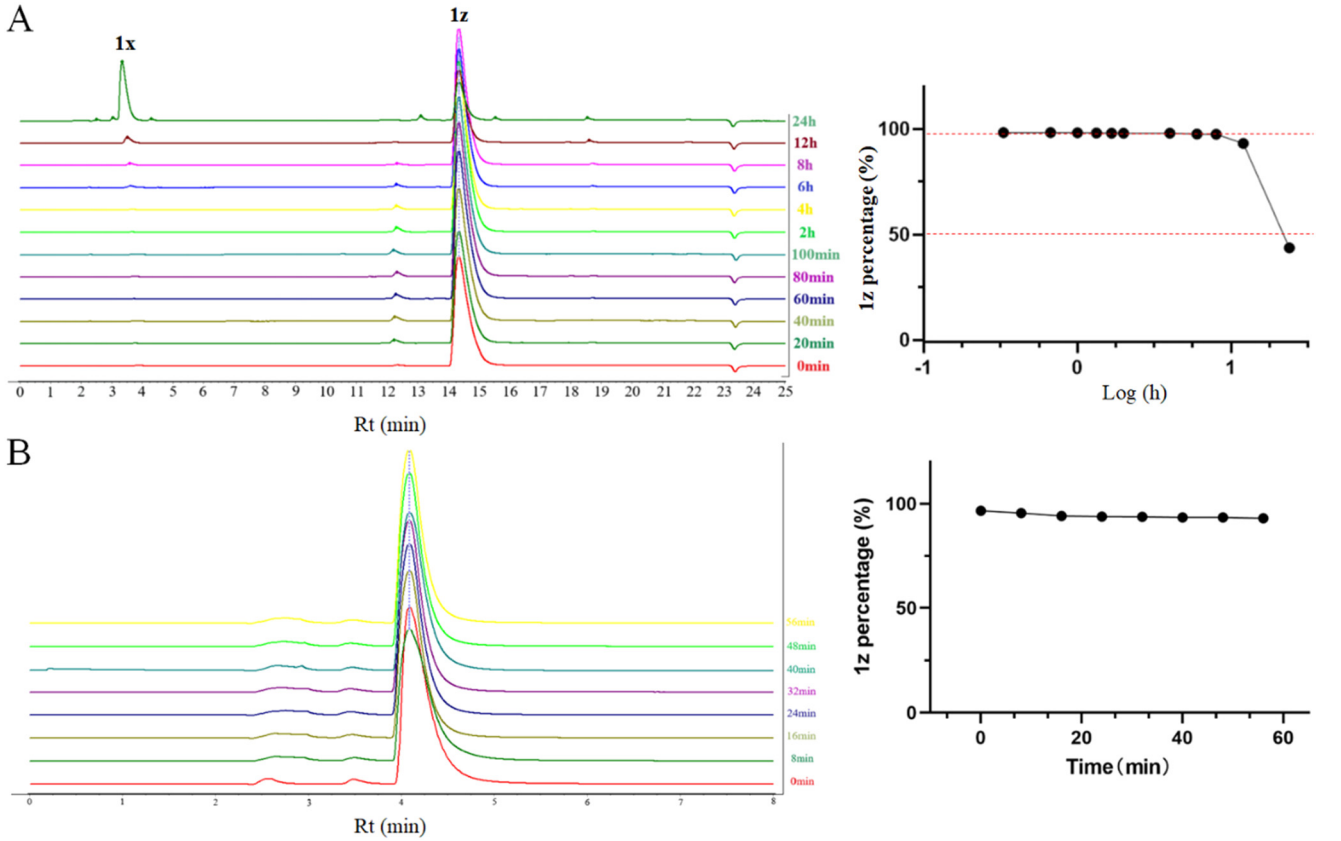

Fig. 8 The percentage of **1z** after heating at 120 °C in toluene for 0–24 h was determined by HPLC (A). The percentage of **1z** after incubating with simulated intestinal fluid at 37 °C for 1 h was determined by HPLC (B).

monitored by analytical thin-layer chromatography (TLC), which was visualized by both ultraviolet light (254 nm) and improved Dragendorff's reagent. THF was distilled from Na, other reagents were obtained commercially. Purification of products was accomplished by flash column chromatography using silica gel (200–300 mesh). All NMR spectra were recorded using a Bruker AVANCE III 500 MHz or AVANCE III 600 MHz (^{1}H NMR) spectrometer and 125 MHz or 150 MHz (^{13}C NMR) in $CDCl_3$: chemical shifts (δ) are given in ppm, coupling constants (J) in Hz, the solvent signals were used as references ($CDCl_3$: δ_C = 77.16 ppm; residual $CHCl_3$ in $CDCl_3$: δ_H = 7.26 ppm).

General procedure for synthesis of enamines 5a–5f. To a solution of corresponding amines **3** (5 mmol) in THF (15 mL) was added NaOH (1.27 mL, 6 N in H_2O, 7.5 mmol) dropwise at 0 °C; the resulting mixture was stirred for 1 h at 0 °C before 4-methoxy-3-butene-2-ketone (**2**) (5 mmol) was added. The resulting mixture was warmed to room temperature and stirred for 12–16 h. After consumption of the starting materials, the reaction was quenched by addition of water (2 mL) and extracted with DCM (6 × 10 mL). The combined organic layer was dried over Na_2SO_4, filtered, and concentrated *in vacuo*. The crude product was purified by silica gel column chromatography (DCM/MeOH = 20 : 1, v/v) to afford enamines **5a–5f.**

(*E*)-4-(4-Methylpiperazin-1-yl)but-3-en-2-one (**5a**) (80% yield). ^{1}H NMR (500 MHz, $CDCl_3$) δ 7.36 (d, J = 13.0 Hz, 1H), 5.27 (d, J = 1.9 Hz, 1H), 5.13 (dd, J = 13.0, 1.9 Hz, 1H), 3.26 (brs, 4H), 2.39 (dd, J = 6.7, 3.4 Hz, 4H), 2.28 (d, J = 2.2 Hz, 3H), 2.06 (d, J = 2.2 Hz, 3H).

(*E*)-4-(Methyl(2-(4-methylpiperazin-1-yl)ethyl)amino)but-3-en-2-one (**5b**) (40% yield). ^{1}H NMR (500 MHz, CD_3OD) δ 7.68 (d, J = 12.5 Hz, 1H), 5.12 (brs, 1H), 3.46 (brs, 2H), 3.18 (brs, 1H), 2.89 (s, 3H), 2.58 (t, J = 6.3 Hz, 4H), 2.50 (brs, 5H), 2.28 (s, 3H), 2.10 (s, 3H).

(*E*)-4-(Methylamino)but-3-en-2-one (**5c**) (quantitative yield). ^{1}H NMR (500 MHz, $CDCl_3$) δ 9.65 (s, 1H), 6.61 (dd, J = 12.8, 7.3 Hz, 1H), 4.97 (d, J = 7.3 Hz, 1H), 2.98 (d, J = 5.0 Hz, 3H), 2.03 (s, 3H).

(*E*)-4-(Diethylamino)but-3-en-2-one (**5d**) (quantitative yield). ^{1}H NMR (500 MHz, $CDCl_3$) δ 7.45 (d, J = 11.5 Hz, 1H), 5.08 (d, J = 12.9 Hz, 1H), 3.20 (brs, 4H), 2.06 (s, 3H), 1.15 (t, J = 6.3 Hz, 6H).

(*E*)-4-((2-Methoxyethyl)(methyl)amino)but-3-en-2-one (**5e**) (85% yield). ^{1}H NMR (500 MHz, $CDCl_3$) δ 7.45 (d, J = 12.6 Hz, 1H), 5.04 (d, J = 12.9 Hz, 1H), 3.53–3.42 (m, 2H), 3.33 (brs, 2H), 3.31 (s, 3H), 2.82 (brs, 3H), 2.06 (s, 3H).

(*E*)-4-((2-(Dimethylamino)ethyl)(methyl)amino)but-3-en-2-one (**5f**) (74% yield). ^{1}H NMR (500 MHz, $CDCl_3$) δ 7.45 (d, J = 12.5 Hz, 1H), 5.06 (d, J = 12.8 Hz, 1H), 3.44 (t, J = 6.5 Hz, 2H), 2.88 (brs, 3H), 2.69 (t, J = 7.0 Hz, 2H), 2.42 (s, 6H), 2.06 (s, 3H).

General procedure for synthesis of aryl/penta-1,4-dien-3-one/amine hybrids 1a–1af. To a solution of corresponding enamines **5** (0.3 mmol) in THF (2 mL) was added dropwise LiHMDS (0.36 mmol) at −78 °C and stirred for 30 min before aldehydes **4** (0.3 mmol in 1 mL THF) was added; then the resulting mixture was warmed to room temperature and stirred for 12–20 h. The reaction was quenched by addition of water (2 mL) and extracted with DCM (10 mL × 5). The combined organic layer was dried over Na_2SO_4, filtered, and concentrated *in vacuo*. The residue was purified by silica gel column chromatography (DCM/MeOH/diethylamine = 100 : 5 : 1, v/v) to afford hybrids **1a–1af**.

(1*E*,4*E*)-1-(3,4-Dimethoxyphenyl)-5-(4-methylpiperazin-1-yl)-penta-1,4-dien-3-one (**1a**) (51% yield); yellow oil. ^{1}H NMR (500 MHz, $CDCl_3$) δ 7.66 (d, J = 12.7 Hz, 1H), 7.49 (d, J = 15.8 Hz, 1H), 7.10 (dd, J = 8.3, 1.8 Hz, 1H), 7.07 (d, J = 1.8 Hz, 1H), 6.83 (d, J = 8.3 Hz, 1H), 6.64 (d, J = 15.8 Hz, 1H), 5.39 (d, J = 12.7 Hz, 1H), 3.89 (s, 3H), 3.88 (s, 3H), 3.37 (brs, 4H), 2.46–2.42 (m, 4H), 2.31 (s, 3H). ^{13}C NMR (125 MHz, $CDCl_3$) δ 187.0, 151.8, 150.4, 149.1, 138.9, 128.7, 126.4, 122.2, 111.1, 109.7, 96.1, 56.0, 55.9, 54.4 (×4), 46.2. HRESI-MS calculated for $[M + H]^+$ $C_{18}H_{25}N_2O_3^+$ (m/z): 317.1860; found: 317.1868. HPLC purity: 99.0% (t_R = 11.03 min).

(1*E*,4*E*)-1-(6-Methoxy-2,3-dihydro-1*H*-inden-5-yl)-5-(4-methylpiperazin-1-yl)penta-1,4-dien-3-one (**1b**) (28% yield); yellow oil. ^{1}H NMR (500 MHz, $CDCl_3$) δ 7.87 (d, J = 16.0 Hz, 1H), 7.65 (d, J = 12.7 Hz, 1H), 7.41 (s, 1H), 6.79 (s, 1H), 6.78 (d, J = 16.0 Hz, 1H), 5.43 (d, J = 12.7 Hz, 1H), 3.84 (s, 3H), 3.38–3.35 (m, 3H), 2.89 (t, J = 7.4 Hz, 2H), 2.84 (t, J = 7.3 Hz, 2H), 2.47–2.41 (m, 4H), 2.32 (s, 3H), 2.09–2.04 (m, 2H). ^{13}C NMR (126 MHz, $CDCl_3$) δ 188.0, 157.5, 151.7, 147.7, 136.1, 134.8, 127.8, 123.6, 122.7, 107.6, 96.2, 55.8, 54.4 (×4), 46.2, 33.7, 32.1, 25.8. HRESI-MS calculated for $[M + H]^+$ $C_{20}H_{27}N_2O_2^+$ (m/z): 327.2067; found: 327.2075. HPLC purity: 99.0% (t_R = 8.83 min).

(1*E*,4*E*)-1-(3-Methoxynaphthalen-2-yl)-5-(4-methylpiperazin-1-yl)penta-1,4-dien-3-one (**1c**) (21% yield); yellow oil. ^{1}H NMR (500 MHz, $CDCl_3$) δ 8.23 (d, J = 8.6 Hz, 1H), 8.17 (d, J = 16.0 Hz, 1H), 7.78 (d, J = 9.0 Hz, 1H), 7.75 (d, J = 8.1 Hz, 1H), 7.69 (d, J = 12.7 Hz, 1H), 7.46 (ddd, J = 8.4, 6.8, 1.3 Hz, 1H), 7.33 (t, J = 7.9 Hz, 1H), 7.24 (d, J = 1.0 Hz, 1H), 7.00 (d, J = 16.0 Hz, 1H), 5.42 (d, J = 12.7 Hz, 1H), 3.95 (s, 3H), 3.36 (brs, 4H), 2.47–2.40 (m, 4H), 2.30 (s, 3H). ^{13}C NMR (150 MHz, $CDCl_3$) δ 187.7, 156.2, 151.9, 133.8, 132.9, 132.3, 130.6, 129.1, 128.5, 127.0, 124.0, 123.8, 118.5, 113.0, 96.7, 56.4, 54.4 (×4), 46.2. HRESI-MS calculated for $[M + H]^+$ $C_{21}H_{25}N_2O_2^+$ (m/z): 337.1911; found: 337.1912. HPLC purity: 97.8% (t_R = 7.27 min).

(1*E*,4*E*)-1-(3-Fluoro-2-methoxyphenyl)-5-(4-methylpiperazin-1-yl)penta-1,4-dien-3-one (**1d**) (55% yield); yellow oil. ^{1}H NMR (500 MHz, $CDCl_3$) δ 7.76 (d, J = 16.0 Hz, 1H), 7.67 (d, J = 12.6 Hz, 1H), 7.31 (d, J = 7.7 Hz, 1H), 7.06–7.00 (m, 1H), 7.00–6.94 (m, 1H), 6.80 (d, J = 16.0 Hz, 1H), 5.39 (d, J = 12.6 Hz, 1H), 3.92 (d, J = 1.6 Hz, 3H), 3.38 (brs, 4H), 2.46–2.42 (m, 4H), 2.31 (s, 3H). ^{13}C NMR (125 MHz, $CDCl_3$) δ 187.0, 156.9, 154.9, 152.2, 146.7, 146.6, 132.6, 132.5, 130.88, 130.9, 130.5, 123.7, 123.6, 123.0 (×2), 117.5, 117.3, 96.1, 61.8 (×2), 54.4 (×2), 54.2 (×2), 46.1. HRESI-MS calculated for $[M + H]^+$ $C_{17}H_{22}FN_2O_2^+$ (m/z): 305.1660; found: 305.1670. HPLC purity: 99.3% (t_R = 5.20 min).

(1*E*,4*E*)-1-(4-Methylpiperazin-1-yl)-5-phenylpenta-1,4-dien-3-one (**1e**) (51% yield); yellow oil. ^{1}H NMR (500 MHz, $CDCl_3$) δ 7.68 (d, J = 12.6 Hz, 1H), 7.56 (d, J = 15.8 Hz, 1H), 7.53 (d, J = 7.0 Hz, 2H), 7.37–7.30 (m, 3H), 6.77 (d, J = 15.8 Hz, 1H), 5.39 (d, J = 12.7 Hz, 1H), 3.38 (brs, 4H), 2.48–2.42 (m, 4H), 2.32 (s, 3H). ^{13}C NMR (125 MHz, $CDCl_3$) δ 186.9, 152.1, 138.9, 135.8, 129.3, 128.8 (×2), 128.3, 128.0 (×2), 96.2, 54.5 (×4), 46.2. HRESI-MS calculated for $[M + H]^+$ $C_{16}H_{21}N_2O^+$ (m/z): 257.1648; found: 257.1650. HPLC purity: 99.3% (t_R = 12.84 min).

(1*E*,4*E*)-1-(4-Chlorophenyl)-5-(4-methylpiperazin-1-yl)penta-1,4-dien-3-one (**1f**) (45% yield); yellow oil. ^{1}H NMR (500 MHz, $CDCl_3$) δ 7.69 (d, J = 12.6 Hz, 1H), 7.50 (d, J = 15.8 Hz, 1H), 7.46 (d, J = 8.6 Hz, 2H), 7.32 (d, J = 8.5 Hz, 2H), 6.73 (d, J = 15.8 Hz, 1H), 5.37 (d, J = 12.6 Hz, 1H), 3.39 (brs, 4H), 2.48–2.43 (m, 4H), 2.33 (s, 3H). ^{13}C NMR (125 MHz, $CDCl_3$) δ 186.5, 152.2, 137.5, 135.2, 134.4, 129.2 (×2), 129.1 (×2), 128.8, 96.2, 54.5 (×4), 46.2. HRESI-MS calculated for $[M + H]^+$ $C_{16}H_{20}ClN_2O^+$ (m/z): 291.1259; found: 291.1260. HPLC purity: 99.3% (t_R = 6.49 min).

4-((1*E*,4*E*)-5-(4-methylpiperazin-1-yl)-3-oxopenta-1,4-dien-1-yl)benzonitrile (**1g**) (29% yield); yellow oil. ^{1}H NMR (500 MHz, $CDCl_3$) δ 7.71 (d, J = 12.6 Hz, 1H), 7.60 (q, J = 8.3 Hz, 4H), 7.51 (d, J = 15.8 Hz, 1H), 6.81 (d, J = 15.8 Hz, 1H), 5.36 (d, J = 12.6 Hz, 1H), 3.39 (brs, 4H), 2.51–2.41 (m, 4H), 2.31 (s, 3H). ^{13}C NMR (150 MHz, $CDCl_3$) δ 185.7, 152.6, 140.3, 136.3, 132.6 (×2), 131.5, 128.3 (×2), 118.8, 112.2, 96.2, 55.0, 53.7, 53.3, 46.1, 45.2. HRESI-MS calculated for $[M + H]^+$ $C_{17}H_{20}N_3O^+$ (m/z): 282.1601; found: 282.1605. HPLC purity: >99.9% (t_R = 11.05 min).

(1*E*,4*E*)-1-(4-Methoxyphenyl)-5-(4-methylpiperazin-1-yl)penta-1,4-dien-3-one (**1h**) (38% yield); yellow oil. ^{1}H NMR (500 MHz, $CDCl_3$) δ 7.66 (d, J = 12.7 Hz, 1H), 7.52 (d, J = 15.8 Hz, 1H), 7.48 (d, J = 8.7 Hz, 2H), 6.88 (d, J = 8.7 Hz, 2H), 6.65 (d, J = 15.8 Hz, 1H), 5.38 (d, J = 12.7 Hz, 1H), 3.82 (s, 3H), 3.42–3.32 (m, 4H), 2.50–2.41 (m, 4H), 2.32 (s, 3H). ^{13}C NMR (125 MHz, $CDCl_3$) δ 187.2, 160.9, 151.8, 138.7, 129.6 (×2), 128.6, 126.2, 114.4 (×2), 96.4, 55.5, 54.5 (×4), 46.2. HRESI-MS calculated for $[M + H]^+$ $C_{17}H_{23}N_2O_2^+$ (m/z): 287.1754; found: 287.1756. HPLC purity: 98.7% (t_R = 13.11 min).

(1*E*,4*E*)-1-(2-Methoxyphenyl)-5-(4-methylpiperazin-1-yl)penta-1,4-dien-3-one (**1i**) (65% yield); yellow oil. ^{1}H NMR (500 MHz, $CDCl_3$) δ 7.86 (d, J = 16.1 Hz, 1H), 7.66 (d, J = 12.7 Hz, 1H), 7.54 (dd, J = 7.6, 1.3 Hz, 1H), 7.33–7.27 (m, 1H), 6.94 (t, J = 7.5 Hz, 1H), 6.89 (d, J = 8.3 Hz, 1H), 6.83 (d, J = 16.0 Hz, 1H), 5.44 (d, J = 12.7 Hz, 1H), 3.87 (s, 3H), 3.43–3.32 (m, 4H), 2.51–2.43 (m, 4H), 2.33 (s, 3H). ^{13}C NMR (125 MHz, $CDCl_3$) δ 187.7, 158.4, 151.8, 134.3, 130.6, 129.2, 128.5, 125.0, 120.8, 111.3, 96.2, 55.6, 54.5 (×4), 46.2. HRESI-MS calculated for $[M + H]^+$ $C_{17}H_{23}N_2O_2^+$ (m/z): 287.1754; found: 287.1752. HPLC purity: 97.5% (t_R = 13.51 min).

(1*E*,4*E*)-1-(2-Methoxy-4-methylphenyl)-5-(4-methylpiperazin-1-yl)penta-1,4-dien-3-one (**1j**) (73% yield); yellow oil. ^{1}H NMR

(500 MHz, $CDCl_3$) δ 7.82 (d, J = 16.0 Hz, 1H), 7.65 (d, J = 12.7 Hz, 1H), 7.43 (d, J = 7.8 Hz, 1H), 6.80 (d, J = 16.0 Hz, 1H), 6.75 (d, J = 7.8 Hz, 1H), 6.70 (s, 1H), 5.43 (d, J = 12.7 Hz, 1H), 3.85 (s, 3H), 3.40–3.33 (m, 4H), 2.47–2.42 (m, 4H), 2.35 (s, 3H), 2.32 (s, 3H). ^{13}C NMR (125 MHz, $CDCl_3$) δ 187.9, 158.3, 151.7, 141.3, 134.4, 128.5, 128.1, 122.0, 121.5, 112.0, 96.1, 55.5, 55.4 (×4), 46.2, 22.0. HRESI-MS calculated for $[M + H]^+$ $C_{18}H_{25}N_2O_2^+$ (m/z): 301.1911; found: 301.1912. HPLC purity: 98.8% (t_R = 6.22 min).

3-Methoxy-4-((1*E*,4*E*)-5-(4-methylpiperazin-1-yl)-3-oxopenta-1,4-dien-1-yl)benzonitrile (**1k**) (51% yield); yellow oil. ^{1}H NMR (500 MHz, $CDCl_3$) δ 7.79 (d, J = 16.0 Hz, 1H), 7.69 (d, J = 12.6 Hz, 1H), 7.58 (d, J = 8.0 Hz, 1H), 7.22 (dd, J = 7.9, 1.1 Hz, 1H), 7.10 (d, J = 1.0 Hz, 1H), 6.86 (d, J = 16.0 Hz, 1H), 5.39 (d, J = 12.6 Hz, 1H), 3.89 (s, 3H), 3.39 (brs, 4H), 2.50–2.43 (m, 4H), 2.32 (s, 3H). ^{13}C NMR (125 MHz, $CDCl_3$) δ 186.5, 157.9, 152.4, 132.1, 131.9, 129.9, 128.8, 124.6, 118.9, 114.1, 113.0, 96.2, 55.9, 54.5 (×4), 46.2. HRESI-MS calculated for $[M + H]^+$ $C_{18}H_{22}N_3O_2^+$ (m/z): 312.1707; found: 312.1708. HPLC purity: 95.5% (t_R = 11.44 min).

(1*E*,4*E*)-1-(2-Methoxy-5-nitrophenyl)-5-(4-methylpiperazin-1-yl)penta-1,4-dien-3-one (**1l**) (44% yield); yellow oil. ^{1}H NMR (500 MHz, $CDCl_3$) δ 8.43 (d, J = 2.7 Hz, 1H), 8.18 (dd, J = 9.1, 2.7 Hz, 1H), 7.82 (d, J = 15.9 Hz, 1H), 7.70 (d, J = 12.6 Hz, 1H), 6.94 (d, J = 9.1 Hz, 1H), 6.88 (d, J = 15.9 Hz, 1H), 5.39 (d, J = 12.6 Hz, 1H), 3.97 (s, 3H), 3.40 (s, 4H), 2.50–2.44 (m, 4H), 2.32 (s, 3H). ^{13}C NMR (125 MHz, $CDCl_3$) δ 186.3, 162.6, 152.3, 141.5, 131.3, 131.2, 125.9 (×2), 123.3, 110.9, 96.6, 56.4, 54.4 (×4), 46.1. HRESI-MS calculated for $[M + H]^+$ $C_{17}H_{22}N_3O_4^+$ (m/z): 322.1605; found: 332.1608. HPLC purity: 97.8% (t_R = 12.45 min).

(1*E*,4*E*)-1-(5-(Dimethylamino)-2-methoxyphenyl)-5-(4-methylpiperazin-1-yl)penta-1,4-dien-3-one (**1m**) (38% yield); yellow oil. ^{1}H NMR (500 MHz, $CDCl_3$) δ 7.81 (d, J = 15.9 Hz, 1H), 7.60 (d, J = 12.7 Hz, 1H), 7.42 (d, J = 8.7 Hz, 1H), 6.69 (d, J = 15.9 Hz, 1H), 6.28 (dd, J = 8.7, 1.8 Hz, 1H), 6.14 (d, J = 1.7 Hz, 1H), 5.42 (d, J = 12.7 Hz, 1H), 3.86 (s, 3H), 3.38–3.31 (m, 4H), 3.00 (s, 6H), 2.46–2.39 (m, 4H), 2.31 (s, 3H). ^{13}C NMR (125 MHz, $CDCl_3$) δ 188.3, 160.0, 152.8, 151.1, 135.2, 130.0, 124.3, 113.2, 104.9, 96.4, 95.0, 55.4, 54.5 (×4), 46.2, 40.4 (×2). HRESI-MS calculated for $[M + H]^+$ $C_{19}H_{28}N_3O_2^+$ (m/z): 330.2176; found: 330.2170. HPLC purity: 96.4% (t_R = 14.66 min).

(1*E*,4*E*)-1-(5-Isopropyl-2-methoxyphenyl)-5-(4-methylpiperazin-1-yl)penta-1,4-dien-3-one (**1n**) (61% yield); yellow oil. ^{1}H NMR (500 MHz, $CDCl_3$) δ 7.84 (d, J = 16.1 Hz, 1H), 7.66 (d, J = 12.7 Hz, 1H), 7.40 (d, J = 2.2 Hz, 1H), 7.15 (dd, J = 8.5, 2.2 Hz, 1H), 6.84 (d, J = 16.1 Hz, 1H), 6.82 (d, J = 8.5 Hz, 1H), 5.46 (d, J = 12.7 Hz, 1H), 3.85 (s, 3H), 3.38 (brs, 4H), 2.84 (dq, J = 13.7, 6.9 Hz, 1H), 2.47–2.43 (m, 4H), 2.32 (s, 3H), 1.22 (d, J = 6.9 Hz, 6H). ^{13}C NMR (125 MHz, $CDCl_3$) δ 187.9, 156.6, 151.8, 141.0, 134.6, 129.0, 128.6, 126.5, 124.4, 111.1, 96.0, 55.7, 54.5 (×4), 46.2, 33.4, 24.3 (×2). HRESI-MS calculated for $[M + H]^+$ $C_{20}H_{29}N_2O_2^+$ (m/z): 329.2224; found: 329.2226. HPLC purity: 98.1% (t_R = 9.32 min).

(1*E*,4*E*)-1-(Benzo[*d*][1,3]dioxol-4-yl)-5-(4-methylpiperazin-1-yl)-penta-1,4-dien-3-one (**1o**) (55% yield); yellow oil. ^{1}H NMR (500 MHz, $CDCl_3$) δ 7.67 (d, J = 12.7 Hz, 1H), 7.48 (d, J = 15.9 Hz, 1H), 6.96 (d, J = 15.8 Hz, 1H), 6.93 (dd, J = 7.6, 1.3 Hz, 1H), 6.83–6.75 (m, 2H), 6.03 (s, 2H), 5.38 (d, J = 12.7 Hz, 1H), 3.38 (s, 4H), 2.51–2.40 (m, 4H), 2.31 (s, 3H). ^{13}C NMR (125 MHz, $CDCl_3$) δ 187.1, 152.1, 147.9, 146.2, 133.4, 131.0, 122.9, 121.8, 118.8, 109.0, 101.3, 96.6, 54.6 (×4), 46.2. HRESI-MS calculated for $[M + H]^+$ $C_{17}H_{21}N_2O_3^+$ (m/z): 301.1547; found: 301.1546. HPLC purity: 99.6% (t_R = 12.96 min).

(1*E*,4*E*)-1-(3,5-Dimethoxyphenyl)-5-(4-methylpiperazin-1-yl)-penta-1,4-dien-3-one (**1p**) (23% yield); yellow oil. ^{1}H NMR (500 MHz, $CDCl_3$) δ 7.69 (d, J = 12.6 Hz, 1H), 7.47 (d, J = 15.8 Hz, 1H), 6.73 (d, J = 15.8 Hz, 1H), 6.69 (s, 1H), 6.69 (s, 1H), 6.45 (t, J = 2.1 Hz, 1H), 5.40 (d, J = 12.6 Hz, 1H), 3.80 (s, 6H), 3.39 (brs, 4H), 2.50–2.41 (m, 4H), 2.33 (s, 3H). ^{13}C NMR (125 MHz, $CDCl_3$) δ 186.9, 161.0 (×2), 152.1, 138.9, 137.8, 128.9, 105.9 (×2), 101.9, 96.1, 55.5, 54.3 (×4), 46.2. HRESI-MS calculated for $[M + H]^+$ $C_{18}H_{25}N_2O_3^+$ (m/z): 317.1860; found: 317.1866. HPLC purity: 99.3% (t_R = 13.06 min).

(1*E*,4*E*)-1-(Benzo[*d*][1,3]dioxol-4-yl)-5-(methylamino)penta-1,4-dien-3-one (**1q**) (20% yield); yellow oil. ^{1}H NMR (600 MHz, $CDCl_3$) δ 10.24 (s, 1H), 7.42 (d, J = 15.9 Hz, 1H), 6.94 (dd, J = 7.9, 0.9 Hz, 1H), 6.88 (d, J = 15.9 Hz, 1H), 6.84 (dd, J = 12.7, 7.2 Hz, 1H), 6.80 (d, J = 7.8 Hz, 1H), 6.77 (dd, J = 7.7, 1.1 Hz, 1H), 6.04 (s, 2H), 5.20 (d, J = 7.1 Hz, 1H), 3.06 (d, J = 4.9 Hz, 3H). ^{13}C NMR (150 MHz, $CDCl_3$) δ 188.2, 155.5, 147.9, 146.1, 132.5, 130.9, 122.8, 121.8, 118.9, 108.9, 101.3, 95.1, 35.6. HRESI-MS calculated for $[M + H]^+$ $C_{18}H_{25}N_2O_3^+$ (m/z): 317.1860; found: 317.1866. HPLC purity: 98.7% (t_R = 12.50 min).

(1*E*,4*E*)-1-(3,5-Dimethoxyphenyl)-5-(methylamino)penta-1,4-dien-3-one (**1r**) (34% yield); yellow oil. ^{1}H NMR (600 MHz, $CDCl_3$) δ 10.22 (s, 1H), 7.39 (d, J = 15.8 Hz, 1H), 6.85 (dd, J = 12.7, 7.1 Hz, 1H), 6.68 (s, 1H), 6.68 (s, 1H), 6.65 (d, J = 15.8 Hz, 1H), 6.44 (t, J = 2.2 Hz, 1H), 5.21 (d, J = 7.1 Hz, 1H), 3.81 (s, 6H), 3.07 (d, J = 5.0 Hz, 3H). ^{13}C NMR (150 MHz, $CDCl_3$) δ 187.9, 161.0 (×2), 155.6, 137.9, 128.7, 105.8 (×2), 101.7, 94.8, 94.8, 55.5 (×2), 35.7. HRESI-MS calculated for $[M + H]^+$ $C_{14}H_{18}NO_3^+$ (m/z): 248.1281; found: 248.1286. HPLC purity: 99.0% (t_R = 12.71 min).

(1*E*,4*E*)-1-(benzo[*d*][1,3]dioxol-4-yl)-5-(diethylamino)penta-1,4-dien-3-one (**1s**) (28% yield); yellow oil. ^{1}H NMR (600 MHz, $CDCl_3$) δ 7.77 (d, J = 12.6 Hz, 1H), 7.48 (d, J = 15.4 Hz, 1H), 7.01–6.91 (m, 2H), 6.84–6.74 (m, 2H), 6.05 (s, 2H), 5.31 (d, J = 12.6 Hz, 1H), 3.38–3.21 (m, 4H), 1.24–1.17 (m, 6H). ^{13}C NMR (150 MHz, $CDCl_3$) δ 186.6, 151.9, 151.9, 147.9, 147.9, 146.1, 133.0, 123.0, 121.8, 119.0, 108.9, 101.3, 50.7, 42.9, 14.9, 11.7. HRESI-MS calculated for $[M + H]^+$ $C_{16}H_{20}NO_3^+$ (m/z): 274.1438; found: 274.1436. HPLC purity: 97.3% (t_R = 6.09 min).

(1*E*,4*E*)-1-(Diethylamino)-5-(3,5-dimethoxyphenyl)penta-1,4-dien-3-one (**1t**) (34% yield); yellow oil. ^{1}H NMR (600 MHz, $CDCl_3$) δ 7.77 (d, J = 12.6 Hz, 1H), 7.48 (d, J = 15.7 Hz, 1H), 6.75 (d, J = 15.7 Hz, 1H), 6.70 (s, 1H), 6.70 (s, 1H), 6.44 (t, J = 2.2 Hz, 1H), 5.32 (d, J = 12.6 Hz, 1H), 3.81 (s, 6H), 3.31 (dd, J = 35.4, 5.6 Hz, 4H), 1.26–1.21 (m, 6H). ^{13}C NMR (150 MHz, $CDCl_3$) δ 186.3, 161.0 (×2), 151.9, 138.4, 138.0, 129.2, 105.8 (×2), 95.9, 101.7, 101.7, 55.5 (×2), 50.8, 42.9, 14.9, 11.7. HRESI-MS calculated for $[M + H]^+$ $C_{17}H_{24}NO_3^+$ (m/z): 290.1751; found: 290.1755. HPLC purity: 97.0% (t_R = 6.31 min).

(1*E*,4*E*)-1-(Benzo[*d*][1,3]dioxol-4-yl)-5-(methyl(2-(4-methylpiperazin-1-yl)ethyl)amino)penta-1,4-dien-3-one (**1u**) (25% yield); yellow oil. ^{1}H NMR (500 MHz, $CDCl_3$) δ 7.75 (d, J = 12.0 Hz, 1H), 7.49 (d, J = 15.9 Hz, 1H), 6.97 (d, J = 15.8 Hz, 1H), 6.94 (d, J = 7.5 Hz, 1H), 6.79 (dt, J = 14.2, 7.3 Hz, 2H), 6.04 (s, 2H), 5.27 (d, J = 12.7 Hz, 1H), 3.37 (s, 3H), 2.89 (brs, 2H), 2.69–2.49 (m, 10H), 2.37 (s, 3H). ^{13}C NMR (125 MHz, $CDCl_3$) δ 186.7, 153.4, 147.9, 146.2, 133.2, 131.1, 127.9, 122.9, 121.9, 118.9, 114.0, 109.0, 101.3, 97.0, 56.3, 55.5, 54.9, 52.5, 45.4, 36.2. HRESI-MS calculated for $[M + H]^+$ $C_{20}H_{28}N_3O_3^+$ (m/z): 358.2125; found: 358.2120. HPLC purity: 99.6% (t_R = 9.08 min).

(1*E*,4*E*)-1-(3,5-Dimethoxyphenyl)-5-(methyl(2-(4-methylpiperazin-1-yl)ethyl)amino)penta-1,4-dien-3-one (**1v**) (22% yield); yellow oil. ^{1}H NMR (500 MHz, $CDCl_3$) δ 7.75 (d, J = 11.8 Hz, 1H), 7.45 (d, J = 15.8 Hz, 1H), 6.73 (d, J = 15.8 Hz, 1H), 6.68 (d, J = 2.2 Hz, 2H), 6.43 (t, J = 2.1 Hz, 1H), 5.27 (d, J = 12.2 Hz, 1H), 3.79 (s, 6H), 3.37 (s, 3H), 2.89 (brs, 2H), 2.70–2.42 (m, 11H), 2.35 (s, 3H). ^{13}C NMR (125 MHz, $CDCl_3$) δ 186.4, 161.0 (×2), 153.4, 138.7, 137.8, 128.9, 105.9 (×2), 101.8, 96.6, 56.5, 55.5 (×2), 54.9 (×4), 52.7, 45.6, 36.3. HRESI-MS calculated for $[M + H]^+$ $C_{21}H_{32}N_3O_3^+$ (m/z): 374.2438; found: 374.2440. HPLC purity: 99.8% (t_R = 13.92 min).

(1*E*,4*E*)-1-(3,5-Dimethoxyphenyl)-5-((2-methoxyethyl)(methyl)-amino)penta-1,4-dien-3-one (**1w**) (39% yield); yellow oil. ^{1}H NMR (500 MHz, $CDCl_3$) δ 7.76 (d, J = 12.5 Hz, 1H), 7.47 (d, J = 15.8 Hz, 1H), 6.75 (d, J = 15.8 Hz, 1H), 6.70 (d, J = 2.0 Hz, 2H), 6.44 (t, J = 2.1 Hz, 1H), 5.30 (d, J = 12.5 Hz, 1H), 3.81 (s, 6H), 3.54 (brs, 2H), 3.43 (brs, 2H), 3.35 (s, 3H), 2.94 (s, 3H). ^{13}C NMR (125 MHz, $CDCl_3$) δ 186.6, 161.1 (×2), 153.3, 138.7, 138.0, 129.0, 106.0 (×2), 101.9, 96.8, 71.3, 59.2, 57.7, 55.5 (×2), 36.7. HRESI-MS calculated for $[M + H]^+$ $C_{17}H_{24}NO_4^+$ (m/z): 306.1700; found: 306.1704. HPLC purity: >99.9% (t_R = 6.05 min).

(1*E*,4*E*)-1-(3-Hydroxyphenyl)-5-(4-methylpiperazin-1-yl)penta-1,4-dien-3-one (**1x**) (45% yield); yellow oil. Compound **1x** was prepared from **1z** by removal of the TBS group under the condition of tetrabutylammonium fluoride (TBAF) (2.0 eq.) in a mixed solvent of THF/AcOH (20 : 1, v/v).[42] ^{1}H NMR (500 MHz, $CDCl_3$) δ 7.72 (d, J = 12.6 Hz, 1H), 7.61 (d, J = 15.7 Hz, 1H), 7.22 (dd, J = 9.1, 6.6 Hz, 2H), 7.09 (d, J = 7.7 Hz, 1H), 6.89 (dd, J = 8.0, 1.8 Hz, 1H), 6.78 (d, J = 15.7 Hz, 1H), 5.39 (d, J = 12.6 Hz, 1H), 3.38 (s, 4H), 2.52–2.39 (m, 4H), 2.33 (s, 3H). ^{13}C NMR (125 MHz, $CDCl_3$) δ 187.3, 157.3, 152.7, 139.7, 136.8, 129.8, 127.9, 119.3, 117.2, 115.4, 96.3, 54.2 (×4), 45.9. HRESI-MS calculated for $[M + H]^+$ $C_{16}H_{21}N_2O_2^+$ (m/z): 273.1598; found: 273.1597. HPLC purity: >99.9% (t_R = 9.46 min).

(1*E*,4*E*)-1-(3-Methoxyphenyl)-5-(4-methylpiperazin-1-yl)penta-1,4-dien-3-one (**1y**) (67% yield); yellow oil. ^{1}H NMR (500 MHz, $CDCl_3$) δ 7.69 (d, J = 12.7 Hz, 1H), 7.53 (d, J = 15.8 Hz, 1H), 7.28 (dd, J = 8.8, 7.0 Hz, 2H), 7.14 (d, J = 7.7 Hz, 1H), 6.89 (dd, J = 8.2, 2.3 Hz, 1H), 6.76 (d, J = 15.8 Hz, 1H), 5.41 (d, J = 12.7 Hz, 1H), 3.83 (s, 3H), 3.40 (brs, 4H), 2.52–2.43 (m, 4H), 2.33 (s, 3H). ^{13}C NMR (125 MHz, $CDCl_3$) δ 186.9, 159.9, 152.1, 138.8, 137.2, 129.8, 128.6, 124.3, 120.7, 115.3, 112.9, 96.2, 55.4, 54.4 (×4), 46.1. HRESI-MS calculated for $[M + H]^+$ $C_{17}H_{23}N_2O_2^+$ (m/z): 287.1754; found: 287.1755. HPLC purity: 99.1% (t_R = 12.74 min).

(1*E*,4*E*)-1-(3-((*Tert*-butyldimethylsilyl)oxy)phenyl)-5-(4-methylpiperazin-1-yl)penta-1,4-dien-3-one (**1z**) (55% yield); yellow oil. ^{1}H NMR (500 MHz, $CDCl_3$) δ 7.68 (d, J = 12.7 Hz, 1H), 7.48 (d, J = 15.8 Hz, 1H), 7.20 (t, J = 7.8 Hz, 1H), 7.13 (d, J = 7.7 Hz, 1H), 7.03–6.97 (m, 1H), 6.83–6.76 (m, 1H), 6.71 (d, J = 15.8 Hz, 1H), 5.39 (d, J = 12.7 Hz, 1H), 3.38 (brs, 4H), 2.48–2.42 (m, 4H), 2.32 (s, 3H), 0.98 (s, 9H), 0.19 (s, 6H). ^{13}C NMR (125 MHz, $CDCl_3$) δ 187.0, 156.1, 152.1, 138.8, 137.4, 129.8, 128.5, 121.3 (×2), 119.4, 96.2, 54.5 (×4), 46.2, 25.8 (×3), 18.4, −4.3 (×2). HRESI-MS calculated for $[M + H]^+$ $C_{22}H_{35}N_2O_2Si^+$ (m/z): 387.2462; found: 387.2466. HPLC purity: 99.2% (t_R = 14.30 min).

(2*Z*,4*E*)-1-(Benzo[*d*][1,3]dioxol-4-yl)-3-hydroxy-5-((2-methoxyethyl)(methyl)amino)penta-2,4-dien-1-one (**1aa**) (24% yield); yellow oil. ^{1}H NMR (500 MHz, $CDCl_3$) δ 7.68 (d, J = 12.6 Hz, 1H), 7.43 (dd, J = 6.6, 2.8 Hz, 1H), 6.91–6.85 (m, 2H), 6.17 (s, 1H), 6.06 (s, 2H), 4.93 (d, J = 12.7 Hz, 1H), 3.53 (s, 2H), 3.41 (s, 2H), 3.35 (s, 3H), 2.88 (d, J = 41.6 Hz, 3H). ^{13}C NMR (125 MHz, $CDCl_3$) δ 188.3, 173.6, 151.4, 148.0, 145.9, 122.1, 121.6, 120.4, 119.1, 110.5, 101.3, 99.2, 94.1, 71.2, 59.2, 57.7, 36.5. HRESI-MS calculated for $[M + H]^+$ $C_{16}H_{20}NO_5^+$ (m/z): 306.1336; found: 306.1338. HPLC purity: >99.9% (t_R = 6.17 min).

(1*E*,4*E*)-1-(4-methylpiperazin-1-yl)-5-(3,4,5-trimethoxyphenyl)-penta-1,4-dien-3-one (**1ab**) (42%); yellow oil. ^{1}H NMR (500 MHz, $CDCl_3$) δ 7.70 (d, J = 12.6 Hz, 1H), 7.47 (d, J = 15.7 Hz, 1H), 6.77 (s, 2H), 6.67 (d, J = 15.7 Hz, 1H), 5.41 (d, J = 12.6 Hz, 1H), 3.87 (s, 6H), 3.86 (s, 3H), 3.41 (brs, 4H), 2.54–2.46 (m, 4H), 2.35 (s, 3H). ^{13}C NMR (125 MHz, $CDCl_3$) δ 186.9, 153.5 (×2), 152.1, 139.6, 139.1, 131.4, 127.8, 105.2 (×2), 96.2, 61.1, 56.2 (×2), 54.3 (×4), 46.0. HRESI-MS calculated for $[M + H]^+$ $C_{16}H_{20}NO_5^+$ (m/z): 306.1336; found: 306.1338. HPLC purity: 99.7% (t_R = 11.19 min).

(1*E*,4*E*)-1-(3,5-Dimethoxyphenyl)-5-((2-(dimethylamino)ethyl)-(methyl)amino)penta-1,4-dien-3-one (**1ac**) (27%); yellow oil. ^{1}H NMR (500 MHz, $CDCl_3$) δ 7.76 (d, J = 11.0 Hz, 1H), 7.46 (d, J = 15.8 Hz, 1H), 6.74 (d, J = 15.8 Hz, 1H), 6.69 (d, J = 1.9 Hz, 2H), 6.44 (s, 1H), 5.29 (d, J = 12.4 Hz, 1H), 3.80 (s, 6H), 3.37 (brs, 2H), 2.91 (brs, 2H), 2.49 (t, J = 6.1 Hz, 2H), 2.26 (s, 6H). ^{13}C NMR (126 MHz, $CDCl_3$) δ 186.5, 161.0 (×2), 153.2, 138.7, 137.9, 129.0, 105.9 (×2), 101.9, 96.7, 58.1, 56.1, 55.5 (×2), 45.7 (×2), 36.2. HRESI-MS calculated for $[M + H]^+$ $C_{18}H_{27}N_2O_3^+$ (m/z): 319.2016; found: 319.2015. HPLC purity: 98.1% (t_R = 9.41 min).

(1*E*,4*E*)-1-(furan-3-yl)-5-(4-methylpiperazin-1-yl)penta-1,4-dien-3-one (**1ad**) (63% yield); yellow oil. ^{1}H NMR (500 MHz, $CDCl_3$) δ 7.66 (d, J = 12.7 Hz, 1H), 7.62 (s, 1H), 7.46 (d, J = 15.7 Hz, 1H), 7.41 (s, 1H), 6.60 (d, J = 1.5 Hz, 1H), 6.51 (d, J = 15.6 Hz, 1H), 5.35 (d, J = 12.7 Hz, 1H), 3.38 (brs, 4H), 2.50–2.41 (m, 4H), 2.33 (s, 3H). ^{13}C NMR (125 MHz, $CDCl_3$) δ 186.8, 151.8, 144.0, 143.9, 128.7, 128.2, 123.4, 107.6, 95.9, 54.3 (×4), 46.0. HRESI-MS calculated for $[M + H]^+$ $C_{14}H_{19}N_2O_2^+$ (m/z): 247.1441; found: 247.1440. HPLC purity: 98.2% (t_R = 9.85 min).

(1*E*,4*E*)-1-(4-Methylpiperazin-1-yl)-5-(thiophen-3-yl)penta-1,4-dien-3-one (**1ae**) (78% yield); yellow oil. ^{1}H NMR (500 MHz, $CDCl_3$) δ 7.66 (d, J = 12.7 Hz, 1H), 7.54 (d, J = 15.7 Hz, 1H), 7.42 (s, 1H), 7.29 (d, J = 1.7 Hz, 2H), 6.59 (d, J = 15.7 Hz, 1H), 5.36

(d, J = 12.7 Hz, 1H), 3.37 (brs, 4H), 2.48–2.41 (m, 4H), 2.31 (s, 3H). ^{13}C NMR (125 MHz, $CDCl_3$) δ 187.1, 152.0, 138.7, 132.6, 128.0, 127.1, 126.6, 125.2, 96.0, 54.9, 53.7, 53.0, 46.2, 45.0. HRESI-MS calculated for $[M + H]^+$ $C_{14}H_{19}N_2OS^+$ (m/z): 263.1213; found: 263.1216. HPLC purity: 95.6% (t_R = 11.78 min).

(1*E*,4*E*)-1-(4-Methylpiperazin-1-yl)-5-(pyridin-3-yl)penta-1,4-dien-3-one (**1af**) (64% yield); yellow oil. ^{1}H NMR (500 MHz, $CDCl_3$) δ 8.76 (s, 1H), 8.54 (s, 1H), 7.81 (d, J = 7.8 Hz, 1H), 7.70 (d, J = 12.5 Hz, 1H), 7.52 (d, J = 15.8 Hz, 1H), 7.28 (s, 1H), 6.81 (d, J = 15.8 Hz, 1H), 5.38 (d, J = 12.6 Hz, 1H), 3.41 (s, 4H), 2.54–2.43 (m, 4H), 2.34 (s, 3H). ^{13}C NMR (150 MHz, $CDCl_3$) δ 186.0, 152.4, 150.0, 149.5, 135.1, 134.3, 131.7, 130.2, 123.9, 96.1, 54.4 (×4), 46.1. HRESI-MS calculated for $[M + H]^+$ $C_{14}H_{19}N_2OS^+$ (m/z): 263.1213; found: 263.1216. HPLC purity: 96.4% (t_R = 7.88 min).

Biology

MTT assay. Cell viability after treatments of tested compounds (20 μM) was evaluated by MTT assay according to our previous work.[42] The IC_{50} values were determined by non-linear regression analysis using GraphPad Prism 5 software.

Fluorescence polarization (FP). HSP90 NTD inhibitory activity was determined by a competitive binding assay against FITC-geldanamycin (GA) according to the literature.[52] The tested compounds were dissolved in DMSO and then appropriately diluted to obtain a gradient concentration (0.03–16.0 μM) for addition to the final reaction system. The HSP90 reaction system consisted of HSP90α (10 nM), BSA (1%), FITC-GA (5 nM), and reaction buffer. After thoroughly mixing all components (DMSO <1%), the reaction system was incubated at room temperature for 3 h. Subsequently, the fluorescence was measured at 485 nm excitation wavelength and 530 nm emission wavelength using a SpectraMax M5 plate reader. HSP90 NTD activity% = (FP_{drug} − $FP_{backgroud}$)/(FP_{enzyme} − $FP_{backgroud}$) × 100%. Curve fitting was performed using GraphPad Prism 5.

AlphaScreen-based HSP90 C-terminal inhibition. The HSP90 C-terminal inhibitory activity was determined by a modified AlphaScreen assay system (PerkinElmer, Waltham, MA) according to our previous work.[42]

Western blot. Cells were digested with trypsin, centrifuged, washed with PBS once before recentrifugation, and lysed in RIPA lysate containing a cocktail of phosphatase and protease inhibitors. The supernatant was collected (14 000 rpm, 4 °C, 15 min) and the protein concentration determined using a BCA reagent kit (Beyotime Shanghai, China). Twenty micrograms protein was separated by SDS-PAGE and transferred to an Immobilon-P Transfer Membrane (Millipore Corporation, Billerica, MA, USA). After blocking in 5% non-fat milk for 1 h at room temperature, the membrane was incubated with primary antibodies overnight at 4 °C; primary antibody dilutions were as follows: HER2 (1 : 1000), AKT (1 : 1000), pAKT (1 : 1000), CDK4 (1 : 1000), HSP70 (1 : 1000), HSP90 (1 : 1000), caspase-3 (1 : 1000), CL-caspase-3 (1 : 1000), PARP (1 : 1000), caspase-8 (1 : 1000), caspase-9 (1 : 1000), and GAPDH (1 : 10000), followed by incubation with HRP-conjugated rabbit or rat secondary antibodies (1 : 1000–1 : 5000). An ECL Chemiluminescence Substrate Kit (Biosharp, Anhui, China) was used for detection.

Cell cycle analysis and annexin V/PI assay. Pancreatic enzyme digestion of cells, centrifugation collection, 70% anhydrous ethanol fixation overnight or longer were performed. Absolute ethanol was washed off and cells were incubated with RNAase (0.2 mg ml^{-1}) and propidium iodide (PI, 0.1 mg mL^{-1}) for 20 min. For the annexin V/PI assay, a FITC-conjugated annexin V apoptosis detection kit (Solarbio, Beijing, China) was used according to the manufacturer's protocol. Stained cells were analyzed by flow cytometry using BD FACS Celesta.

Immunofluorescence analysis. For immunofluorescence analysis, cells were seeded in a 24-well plate that was previously inserted into the cell ladder and then treated with the tested compounds. The cells were washed twice with PBS in a warm bath and fixed with 4% paraformaldehyde for 15 min, permeabilized with 0.2% Triton X-100 for 5 min, followed by blocking with BSA (3%, 15 min), and then incubated with primary antibody (1 h, room temperature) and fluorescein-conjugated secondary antibody (1 h, room temperature). Cells were mounted with antifade mounting medium with DAPI (Beyotime Shanghai, China) and images were obtained using a Zeiss upright fluorescence microscope.

Molecular modeling. The ligand (**1z**) and receptor (PDB 3Q6M)[47] were prepared using Autodock Tools v1.56 (ref. 53) according to our previous work.[42] A grid box that covered the whole HSP90 C-terminus in 3Q6M was chosen. Docking parameters were set as the default values. Docking conformations were classified into different clusters by binding energy, and the cluster with the lowest binding energy was selected. In the selected cluster, conformations with the lowest binding energy and RMSD (<2.0 Å) were finally chosen to analyze the receptor–ligand interaction.

Stability. Thermostability was tested using **1z** (1 mg mL^{-1}) in boiling toluene (distilled); the remaining percentage of **1z** was detected by an HPLC instrument (Agilent 1260) equipped with an Eclipse XDB-C18 (5 μm, 4.6 mm × 250 mm) column after the appointed time. HPLC analysis method A: 0.00–2.00 min: 70% MeOH/30% H_2O; 2.01–15.00 min: from 70% MeOH/30% H_2O to 100% MeOH; 15.00–20.00 min: 100% MeOH; 20.01–25.00 min: 70% MeOH/30% H_2O; method B: 0.00–2.00 min: 45% MeOH/55% H_2O; 2.01–15.00 min: from 45% MeOH/55% H_2O to 100% MeOH; 15.00–20.00 min: 100% MeOH; 20.01–25.00 min: 45% MeOH/55% H_2O.

In vitro metabolic stability was tested in simulated intestinal fluid (Phygene) which was incubated with **1z** (1 mg mL^{-1}); the remaining percentage of **1z** was detected by an HPLC instrument (Agilent 1260) equipped with an Eclipse XDB-C18 (5 μm, 4.6 mm × 250 mm) column after the appointed time. HPLC analysis method: 95% MeOH/5% H_2O.

Author contributions

Yu-Ting Liao, Xin-Ye Du, and Mei Wang: investigation and writing – original draft. Chun-Xia Zheng: software. Dashan Li: data curation. Chuan-Huizi Chen: methodology, formal analysis. Rong-Tao Li: writing – review & editing, supervision, resources. Li-Dong Shao: conceptualization, project administration, resources, supervision, writing – original draft, writing – review & editing.

Conflicts of interest

The authors declare that they have no known conflicts of interest.

Acknowledgements

The authors are grateful for the financial support from the National Natural Science Foundation of China (81960631, 82260683, and 22067012), the Yunnan Fundamental Research Project (202001AS070038), the Top Young Talent of Ten Thousand Talents Program of Yunnan Province (D. L. and L.-D. S.), the Bioactive Ethnopharmacol Molecules Chemical Conversion and Application Innovation Team of the Department of Education of Yunnan Province (2022), and the Start-up Fund of Yunnan University of Chinese Medicine (2019YZG03).

References

1 H. Sung, J. Ferlay, R. L. Siegel, M. Laversanne, I. Soerjomataram, A. Jemal and F. Bray, *Ca-Cancer J. Clin.*, 2021, **71**, 209–249.
2 A. N. Giaquinto, H. Sung, K. D. Miller, J. L. Kramer, L. A. Newman, A. Minihan, A. Jemal and R. L. Siegel, *Ca-Cancer J. Clin.*, 2022, **72**, 524–541.
3 R. Zheng, S. Zhang, H. Zeng, S. Wang, K. Sun, R. Chen, L. Li, W. Wei and J. He, *J. Natl. Cancer Inst.*, 2022, **2**, 1–9.
4 G.-T. Lang, Y.-Z. Jiang, J.-X. Shi, F. Yang, X.-G. Li, Y.-C. Pei, C.-H. Zhang, D. Ma, Y. Xiao, P.-C. Hu, H. Wang, Y.-S. Yang, L.-W. Guo, X.-X. Lu, M.-Z. Xue, P. Wang, A. Y. Cao, H. Ling, Z.-H. Wang, K.-D. Yu, G.-H. Di, D.-Q. Li, Y.-J. Wang, Y. Yu, L.-M. Shi, X. Hu, W. Huang and Z.-M. Shao, *Nat. Commun.*, 2020, **11**, 5679.
5 S. Park, Y.-J. Kim, J. M. Park, M. Park, K. D. Nam, L. Farrand, C.-T. Nguyen, M. T. La, J. Ann, J. Lee, J. Y. Kim and J. H. Seo, *Cell Death Discovery*, 2021, **7**, 354.
6 J. M. Park, Y.-J. Kim, S. Park, M. Park, L. Farrand, C.-T. Nguyen, J. Ann, G. Nam, H.-J. Park, J. Lee, J. Y. Kim and J. H. Seo, *Mol. Cancer*, 2020, **19**, 161.
7 L. B. Peterson and B. S. Blagg, *Future Med. Chem.*, 2009, **1**, 267–283.
8 R. L. Matts, A. Dixit, L. B. Peterson, L. Sun, S. Voruganti, P. Kalyanaraman, S. D. Hartson, G. M. Verkhivker and B. S. J. Blagg, *ACS Chem. Biol.*, 2011, **6**, 800–807.
9 L. Li, L. Wang, Q.-D. You and X.-L. Xu, *J. Med. Chem.*, 2020, **63**, 1798–1822.
10 E. Amatya and B. S. J. Blagg, *Bioorg. Med. Chem. Lett.*, 2023, **80**, 129111.
11 J. Yu, C. Zhang and C. Song, *Eur. J. Med. Chem.*, 2022, **238**, 114516.
12 J. Trepel, M. Mollapour, G. Giaccone and L. Neckers, *Nat. Rev. Cancer*, 2010, **10**, 537–549.
13 J. Koren and B. S. J. Blagg, in *HSF1 and Molecular Chaperones in Biology and Cancer*, ed. M. L. Mendillo, D. Pincus and R. Scherz-Shouval, Springer International Publishing, Cham, 2020, pp. 135–146, DOI: **10.1007/978-3-030-40204-4_9**.
14 D. Bickel and H. Gohlke, *Bioorg. Med. Chem.*, 2019, **27**, 115080.
15 J. A. Burlison, L. Neckers, A. B. Smith, A. Maxwell and B. S. J. Blagg, *J. Am. Chem. Soc.*, 2006, **128**, 15529–15536.
16 G. Shen, X. M. Yu and B. S. J. Blagg, *Bioorg. Med. Chem. Lett.*, 2004, **14**, 5903–5906.
17 X. M. Yu, G. Shen, L. Neckers, H. Blake, J. Holzbeierlein, B. Cronk and B. S. J. Blagg, *J. Am. Chem. Soc.*, 2005, **127**, 12778–12779.
18 A. C. Donnelly, J. R. Mays, J. A. Burlison, J. T. Nelson, G. Vielhauer, J. Holzbeierlein and B. S. J. Blagg, *J. Org. Chem.*, 2008, **73**, 8901–8920.
19 J. A. Burlison, C. Avila, G. Vielhauer, D. J. Lubbers, J. Holzbeierlein and B. S. J. Blagg, *J. Org. Chem.*, 2008, **73**, 2130–2137.
20 J. R. Mays, S. A. Hill, J. T. Moyers and B. S. J. Blagg, *Bioorg. Med. Chem.*, 2010, **18**, 249–266.
21 L. B. Peterson and B. S. J. Blagg, *Bioorg. Med. Chem. Lett.*, 2010, **20**, 3957–3960.
22 H. Zhao, A. C. Donnelly, B. R. Kusuma, G. E. L. Brandt, D. Brown, R. A. Rajewski, G. Vielhauer, J. Holzbeierlein, M. S. Cohen and B. S. J. Blagg, *J. Med. Chem.*, 2011, **54**, 3839–3853.
23 B. R. Kusuma, A. S. Duerfeldt and B. S. J. Blagg, *Bioorg. Med. Chem. Lett.*, 2011, **21**, 7170–7174.
24 H. Zhao and B. S. J. Blagg, *Bioorg. Med. Chem. Lett.*, 2013, **23**, 552–557.
25 B. R. Kusuma, A. Khandelwal, W. Gu, D. Brown, W. Liu, G. Vielhauer, J. Holzbeierlein and B. S. J. Blagg, *Bioorg. Med. Chem.*, 2014, **22**, 1441–1449.
26 K. M. Byrd, C. Subramanian, J. Sanchez, H. F. Motiwala, W. Liu, M. S. Cohen, J. Holzbeierlein and B. S. J. Blagg, *Chem. – Eur. J.*, 2016, **22**, 6921–6931.
27 G. Garg, L. K. Forsberg, H. Zhao and B. S. J. Blagg, *Chem. – Eur. J.*, 2017, **23**, 16574–16585.
28 L. K. Forsberg, R. E. Davis, V. K. Wimalasena and B. S. J. Blagg, *Bioorg. Med. Chem.*, 2018, **26**, 3096–3110.
29 K. W. Pugh, Z. Zhang, J. Wang, X. Xu, V. Munthali, A. Zuo and B. S. J. Blagg, *ACS Med. Chem. Lett.*, 2020, **11**, 1535–1538.
30 C.-T. Nguyen, M. Thanh La, J. Ann, G. Nam, H.-J. Park, J. Min Park, Y.-J. Kim, J. Young Kim, J. Hong Seo and J. Lee, *Bioorg. Med. Chem. Lett.*, 2021, **45**, 128134.
31 S.-C. Lee, H.-Y. Min, H. Choi, H. S. Kim, K.-C. Kim, S.-J. Park, M. A. Seong, J. H. Seo, H.-J. Park, Y.-G. Suh, K.-W. Kim,

H.-S. Hong, H. Kim, M.-Y. Lee, J. Lee and H.-Y. Lee, *Mol. Pharmacol.*, 2015, **88**, 245–255.
32 H. S. Kim, M. Hong, J. Ann, S. Yoon, C.-T. Nguyen, S.-C. Lee, H.-Y. Lee, Y.-G. Suh, J. H. Seo, H. Choi, J. Y. Kim, K.-W. Kim, J. Kim, Y.-M. Kim, S.-J. Park, H.-J. Park and J. Lee, *Bioorg. Med. Chem.*, 2016, **24**, 6082–6093.
33 T.-M. Cho, J. Y. Kim, Y.-J. Kim, D. Sung, E. Oh, S. Jang, L. Farrand, V.-H. Hoang, C.-T. Nguyen, J. Ann, J. Lee and J. H. Seo, *Cancer Lett.*, 2019, **447**, 141–153.
34 H. S. Kim, V.-H. Hoang, M. Hong, K. C. Kim, J. Ann, C.-T. Nguyen, J. H. Seo, H. Choi, J. Yong Kim, K.-W. Kim, W. Sub Byun, S. Lee, S. Lee, Y.-G. Suh, J. Chen, H.-J. Park, T.-M. Cho, J. Y. Kim, J. H. Seo and J. Lee, *Bioorg. Med. Chem.*, 2019, **27**, 1370–1381.
35 C.-T. Nguyen, J. Ann, R. Sahu, W. S. Byun, S. Lee, G. Nam, H.-J. Park, S. Park, Y.-J. Kim, J. Y. Kim, J. H. Seo and J. Lee, *Bioorg. Med. Chem. Lett.*, 2020, **30**, 127374.
36 L. D. Alexander, R. P. Sellers, M. R. Davis, V. C. Ardi, V. A. Johnson, R. C. Vasko and S. R. McAlpine, *J. Med. Chem.*, 2009, **52**, 7927–7930.
37 R. C. Vasko, R. A. Rodriguez, C. N. Cunningham, V. C. Ardi, D. A. Agard and S. R. McAlpine, *ACS Med. Chem. Lett.*, 2010, **1**, 4–8.
38 V. C. Ardi, L. D. Alexander, V. A. Johnson and S. R. McAlpine, *ACS Chem. Biol.*, 2011, **6**, 1357–1366.
39 Y. C. Koay, J. R. McConnell, Y. Wang, S. J. Kim, L. K. Buckton, F. Mansour and S. R. McAlpine, *ACS Med. Chem. Lett.*, 2014, **5**, 771–776.
40 M. N. Rahimi, L. K. Buckton, S. S. Zaiter, J. Kho, V. Chan, A. Guo, J. Konesan, S. Kwon, L. K. O. Lam, M. F. Lawler, M. Leong, G. D. Moldovan, D. A. Neale, G. Thornton and S. R. McAlpine, *ACS Med. Chem. Lett.*, 2018, **9**, 73–77.
41 L. Li, N. Chen, D. Xia, S. Xu, W. Dai, Y. Tong, L. Wang, Z. Jiang, Q. You and X. Xu, *Cell Chem. Biol.*, 2021, **28**, 1446–1459.e1446.
42 L.-D. Shao, J. Su, B. Ye, J.-X. Liu, Z.-L. Zuo, Y. Li, Y.-Y. Wang, C. Xia and Q.-S. Zhao, *J. Med. Chem.*, 2017, **60**, 9053–9066.
43 Y. Fukuyama, M. Kubo, T. Esumi, K. Harada and H. Hioki, *Heterocycles*, 2010, **81**, 1571–1602.
44 B. Salehi, Z. Stojanović-Radić, J. Matejić, M. Sharifi-Rad, N. V. A. Kumar, N. Martins and J. Sharifi-Rad, *Eur. J. Med. Chem.*, 2019, **163**, 527–545.
45 P. L. Tran, S.-A. Kim, H. S. Choi, J.-H. Yoon and S.-G. Ahn, *BMC Cancer*, 2010, **10**, 276.
46 O. W. Mak, N. Sharma, J. Reynisson and I. K. H. Leung, *Bioorg. Med. Chem. Lett.*, 2021, **38**, 127857.
47 S. Bhatia, L. Spanier, D. Bickel, N. Dienstbier, V. Woloschin, M. Vogt, H. Pols, B. Lungerich, J. Reiners, N. Aghaallaei, D. Diedrich, B. Frieg, J. Schliehe-Diecks, B. Bopp, F. Lang, M. Gopalswamy, J. Loschwitz, B. Bajohgli, J. Skokowa, A. Borkhardt, J. Hauer, F. K. Hansen, S. H. J. Smits, J. Jose, H. Gohlke and T. Kurz, *ACS Cent. Sci.*, 2022, **8**, 636–655.
48 N. F. Lazareva, V. P. Baryshok and I. M. Lazarev, *Arch. Pharm.*, 2018, **351**, e1700297.
49 M. K. Kurop, C. M. Huyen, J. H. Kelly and B. S. J. Blagg, *Eur. J. Med. Chem.*, 2021, **226**, 113846.
50 J. R. McConnell, L. A. Alexander and S. R. McAlpine, *Bioorg. Med. Chem. Lett.*, 2014, **24**, 661–666.
51 L.-D. Shao, Y. Chen, M. Wang, N. Xiao, Z.-J. Zhang, D. Li and R.-T. Li, *Org. Chem. Front.*, 2022, **9**, 2308–2315.
52 A. Khandelwal, C. N. Kent, M. Balch, S. Peng, S. J. Mishra, J. Deng, V. W. Day, W. Liu, C. Subramanian, M. Cohen, J. M. Holzbeierlein, R. Matts and B. S. J. Blagg, *Nat. Commun.*, 2018, **9**, 425.
53 G. M. Morris, R. Huey, W. Lindstrom, M. F. Sanner, R. K. Belew, D. S. Goodsell and A. J. Olson, *J. Comput. Chem.*, 2009, **30**, 2785–2791.